Quantum Error Correction for Quantum Memories

Barbara M. Terhal

Institute for Quantum Information, RWTH Aachen University, Aachen, Germany

(Dated: June 10, 2014)

This is a pedagogical review of the formalism of qubit stabilizer codes and their possible use in protecting quantum information. We discuss several codes of particular physical interest, e.g. encoding a qubit in an oscillator, 2D topological error correction and 2D subsystem codes. The emphasis in this review is on the use of such codes as a quantum memory.

CONTENTS

I. INTRODUCTION

When the idea of a quantum computer took hold in the '90s it was immediately realized that its implementation would require some form of robustness and error correction. Alexei Kitaev proposed a scheme in which the physical representation of quantum information and realization of logical gates would be naturally robust due to the topological nature of the 2D physical system (Kitaev, 2003). Around the same time Peter Shor formulated a first quantum error-correcting code and proved that a quantum computer could be made fault-tolerant (Shor, 1996). Several authors then established the fault-tolerance threshold theorem (see Theorem 1) which shows that in principle one can realize almost noise-free quantum computation using noisy cmponents at the cost of moderate overhead.

In this review we will discuss the basic ideas behind active quantum error correction with stabilizer codes for the purpose of making a quantum memory. In such a quantum memory, quantum information is distributed among many elementary degrees of freedom, e.g. qubits, such that the dominant noise processes affect this information in a reversible manner, meaning that there exists an error reversal procedure by which one can detect and correct the errors. The choice of how to represent the quantum information in the state space of many elementary qubits is made through the choice of quantum error correcting code.

In Section II.A we start by discussing Shor's code as the most basic example of a quantum error correction code. Using Shor's code we can illustrate the ideas behind the general framework of stabilizer codes (Gottesman, 1997), including subsystem stabilizer codes. For stabilizer and subsystem stabilizer codes on qubits we show explicitly how errors can be detected and subsequently corrected. In section II.A.2 we will also discuss other small examples of quantum error correcting codes and the construction due to Calderbank, Steane and Shor by which two classical codes can be used to construct one quantum code. In Section II.B we widen our perspective beyond stabilizer codes and discuss the general quantum error-correcting conditions as well as some codes which encode qubit(s) into bosonic mode(s) (oscillators). In Section II.C we define D-dimensional stabilizer codes and give various examples of such codes.

As the procedure of detecting and correcting errors itself is subject to noise, the existence of quantum error correcting codes is not sufficient to enable storage or computation of quantum information with arbitrary small error rate. In Section II.D we briefly review how one can, through code concatenation, arrive at the fault-tolerance threshold Theorem. In Section II.D we also discuss vari-

ous proposals for realizing quantum error correction, including the idea of dissipative engineering. The topic of the realization of quantum error correction is again picked up in Section III.D, but in the later section the emphasis is on D-dimensional (topological) codes. In the last section of our introductory Chapter, Section II.E, we review constructions for obtaining a universal set of logical gates for qubits encoded with stabilizer codes and partially motivate our focus on 2D topological stabilizer codes for the use as a quantum memory. This motivation also stems from the fact that the demands on error decoding are much easier to meet for a quantum memory than for universal quantum computation, see Section II.E.

For stationary, non-flying, qubits, an important family of codes are quantum codes in which the elementary qubits can be laid out on a two-dimensional plane such that only local interactions between small numbers of nearest-neighbor qubits in the plane are required for quantum error correction. The practical advantage of such 2D geometry over an arbitrary qubit interaction-structure is that no additonal noisy operations need to be performed to move qubits around. Elementary solid-state qubits require various classical electric or magnetic control fields per qubit, both for defining the qubit subspace and/or for single- and two qubit control and measurement. The simultaneous requirement that qubits can interact sufficiently strongly and that space is available for these control lines imposes technological design constraints, see e.g. (Levy *et al.*, 2009). A two-dimensional layout can be viewed as a compromise between the constraints coming from coding theory, –quantum error correcting codes defined on one-dimensional lines have poor error-correcting properties (Section II.C), and control-line and material fabrication constraints which favor 2D structures over 3D or non-local interaction structures.

These considerations are the reason that we focus in Section III on 2D (topological) codes, in particular the family of 2D topological surface codes which has many favorable properties. For the surface code we show explicitly in Section III.A how logical qubits can be defined, how they can be error-corrected and the noise threshold of this coding scheme. We review two possible ways of encoding qubits in the surface code and performing a CNOT gate (and Hadamard gate) in a way which does not require more qubit resources nor a different noise threshold as compared to a pure quantum memory. In Section III.A.3 we connect to the bosonic code defined in Section II.B by showing how one can concatenate this bosonic code with the surface code or alternatively describe the entire code as a surface code with harmonic oscillators. In Sections III.B and III.C we review two interesting alternatives to the surface code which are the non-topological Bacon-Shor code and a subsystem version of the surface code. Section III.D discusses the physical locality of the process of decoding as well as recent ideas on the realization of so-called direct parity measurements. We conclude our review with a discussion on some practical challenges for quantum error correction.

We recommend the book (Lidar and Brun, 2013) as a broad, comprehensive, reference on quantum error correction.

A. Error Mitigation

Active quantum error correction is not the only way to improve the coherence properties of elementary physical quantum systems and various well-known methods of error mitigation exist. In a wide variety of systems there is classical 1/f noise affecting the parameters of the qubit with a noise power spectral density $S(\omega) \sim 1/\omega^{\alpha}$, $\alpha \approx 1$, favoring slow fluctuations of those parameters (Weissman, 1988) which lead to qubit dephasing. Standard NMR techniques (Vandersypen and Chuang, 2005) have been adapted in such systems to average out these fluctuations using rapid pulse sequences (e.g. spin-echo). More generally, dynamical decoupling is a technique by which the undesired coupling of qubits to other quantum systems can be averaged out through rapid pulse sequences (Lidar, 2012). Aside from actively canceling the effects of noise, one can also try to encode quantum information in so-called decoherence-free subspaces which are effectively decoupled from noise; a simple example is the singlet state $\frac{1}{\sqrt{2}}(|\uparrow,\downarrow\rangle - |\downarrow,\uparrow\rangle)$ which is invariant under a joint (unkown) evolution $U \otimes U$.

A different route towards protecting quantum information is based on passive Hamiltonian engineering. In this approach quantum information is encoded in an eigenspace, typically groundspace, of a many-body, topologically-ordered, Hamiltonian. In this approach no physical mechanisms which actively (and continuously) remove error excitations are invoked. One may consider how to engineer a physical system such that it has efffective, say, 4-body Hamiltonian interactions of the surface code, Section III.A, between nearby qubits in a 2D array (Kitaev, 2006). The strength of this approach is that the protection is built into the hardware instead of being imposed dynamically, negating for example the need for control lines for time-dependent pulses. The challenge of this approach is that it requires lower-body (one-, two- and three-body) terms in the effective Hamiltonian to be small: the elementary qubits of the many-body system should therefore have approximately degenerate levels $|0\rangle$ and $|1\rangle$. However, in order to encode information in, say, the ground-space of such Hamiltonian, one will need to lift this degeneracy to be able to address these levels. Another challenging aspect of such Hamiltonian engineering is that the desired, say, 4-body interactions will be typically be arrived at perturbatively. This means that their strength and therefore the gap of the topologically-ordered Hamiltonian compared with

the temperature T may be small leading to inevitable error excitations. (Douçot and Ioffe, 2012) reviews several ideas for the topological protection of quantum information in superconducting systems while (Gladchenko *et al.*, 2009) demonstrates their experimental feasibility. Another example is the proposal to realize the parity checks of the surface code through Majorana fermion tunneling between 2D arrays of superconducting islands, each supporting 4 Majorana bound states with fixed parity (Terhal *et al.*, 2012).

The information stored in such passive, topologically-ordered many-body system is, at sufficiently low-temperature, protected by a non-zero energy gap for excited states. Research has been devoted to the question whether the $T = 0$ topological phase, characterized by a topological order-parameter, can genuinely extend to non-zero temperature $T > 0$. The same question has also been approached from a dynamical perspective with the notion of a self-correcting quantum memory (Bacon, 2006). A self-correcting quantum memory is a quantum memory in which the accumulation of error excitations over time, which can in turn lead to logical errors corrupting the quantum memory, is energetically (or entropically) disfavored due the presence of macroscopic energy barriers. A qubit encoded in such quantum memory should have a coherence time $\tau(T, n)$ which grows with the size n, –the elementary qubits of the memory–, for temperature $0 < T < T_c$. A 4-dimensional version of the toric code has been shown to be a good example of such finite-temperature topological order or self-correcting memory, see (Alicki *et al.*, 2008; Dennis *et al.*, 2002). One important finding concerning self-correcting quantum memories is that a finite temperature 'quantum memory phase' based on macroscopic energy barriers is unlikely to exist for genuinely local 2D quantum systems. We refer to e.g. (Wootton, 2012) and references therein for an overview of results in this area of research.

B. Some Experimental Advances

Experimental efforts have not advanced into the domain of *scalable* quantum error correction. Scalable quantum error correction would mean (1) making encoded qubits with decoherence rates which are genuinely below that of the elementary qubit and (2) demonstrate how, by increasing coding overhead, one can reach even lower decoherence rates, scaling in accordance with the theory of quantum error correction.

Several experiments exist of the 3-qubit (or 5-qubit) repetition code in liquid NMR, ion-trap, optical and superconducting qubits. Four qubit stabilizer pumping has been realized in ion-trap qubits (Barreiro *et al.*, 2011). Some topological quantum error correction has been implemented with eight-photon cluster states in (Yao *et al.*, 2012) and a continuous-variable version of Shor's 9-qubit code was implemented with optical beams (Aoki *et al.*, 2009). The book (Lidar and Brun, 2013) has a chapter with an overview of experimental quantum error correction. Given the advances in coherence times and ideas of multi-qubit scalable design, in particular in ion-trap and superconducting qubits e.g. (Barends *et al.*, 2014), one may hope to see scalable error correction, fine-tuned to experimental capabilities and constraints, in the years to come.

II. CONCEPTS OF QUANTUM ERROR CORRECTION

A. Shor's Code and The Stabilizer Formalism

The smallest classical code which can correct a single bit-flip error (represented by Pauli X [1]) is the 3-(qu)bit repetition code where we encode $|\overline{0}\rangle = |000\rangle$ and $|\overline{1}\rangle = |111\rangle$. A single error can be corrected by taking the majority of the three bit values and flipping the bit which is different from the majority. In quantum error correction we don't want to measure the 3 qubits to take a majority vote, as we would immediately loose the quantum information represented in the phase and amplitude of an encoded state $|\overline{\psi}\rangle = \alpha|\overline{0}\rangle + \beta|\overline{1}\rangle$.

But we can imagine measuring the parity checks Z_1Z_2 and Z_2Z_3 *without learning the state of each individual qubit*. Fig. 1(a) shows the quantum circuit which measures a parity check represented by a Pauli operator P using an ancilla qubit. Other than giving us parity information, the ideal parity measurement also provides a discretization of errors which is not naturally present in elementary quantum systems. Through interaction with classical or quantum systems the amplitude and phase of a qubit will fluctuate over time: bare quantum information encoded in atomic, photonic, spin or other single quantum systems is barely information as it is undergoing continuous changes. An ideal parity measurement discretizes this continuum of errors into a discrete set of a Pauli errors (X, Y, Z or I on each qubit) which are amenable to correction. If the parity checks Z_1Z_2 and Z_2Z_3 have eigenvalues $+1$, one concludes no error. An outcome of, say, $Z_1Z_2 = -1$ and $Z_2Z_3 = 1$ is consistent with the erred state $X_1|\overline{\psi}\rangle$ where $|\overline{\psi}\rangle$ is any encoded state.

Let us informally introduce some of the notions used in describing a quantum (stabilizer) code. For a code C encoding k qubits, one defines k pairs of logical Pauli operators $(\overline{X}_i, \overline{Z}_i)$, $i = 1, \ldots k$, such that $\overline{X}_i\overline{Z}_i = -\overline{Z}_i\overline{X}_i$ while logical Pauli operators with labels i and i' mutually

[1] Pauli $\sigma_x \equiv X = \begin{pmatrix} 0 & 1 \\ 1 & 0 \end{pmatrix}$, $\sigma_z \equiv Z = \begin{pmatrix} 1 & 0 \\ 0 & -1 \end{pmatrix}$ and $\sigma_y \equiv Y = \begin{pmatrix} 0 & -i \\ i & 0 \end{pmatrix} = iXZ$.

commute (realizing the algebra of Pauli operators acting on k qubits). For the 3-qubit code we have $\overline{X} = X_1X_2X_3$ and $\overline{Z} = Z_1$.

The *code space* of a code C encoding k qubits is spanned by the codewords $|\overline{x}\rangle$ where x is a k-bitstring. All states in the codespace obey the parity checks, meaning that the parity check operators have eigenvalue $+1$ for all states in the code space. In other words, the parity checks act trivially on the codespace. The logical operators of a quantum error-correcting code are non-unique as we can multiply them by the trivially-acting parity check operators to obtain equivalent operators. For example, $\overline{Z}$ for the 3-qubit code is either Z_1 or Z_2, or Z_3 or $Z_1Z_2Z_3$.

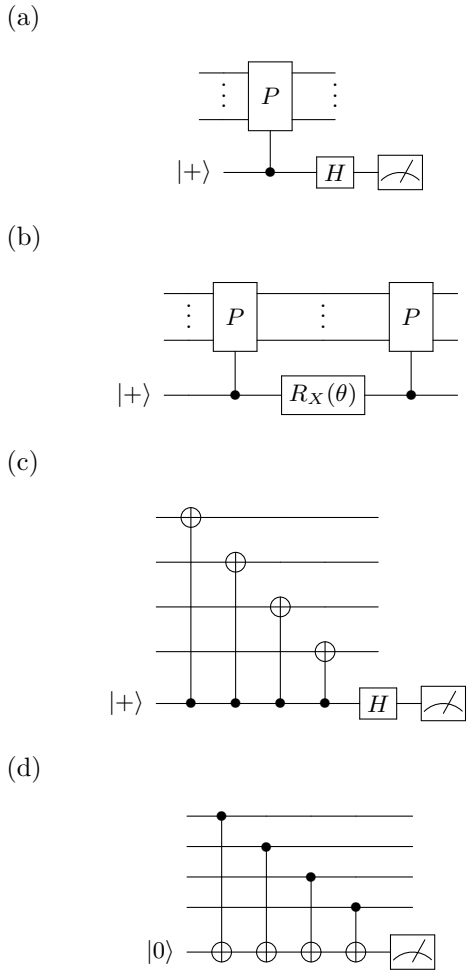

FIG. 1 Measuring parity checks the quantum-circuit way. The meter denotes measurement in the $\{|0\rangle, |1\rangle\}$ basis or M_Z. (a) Circuit to measure the ± 1 eigenvalues of a unitary multi-qubit Pauli operator P. The gate is the controlled-P gate which applies P when the control qubit is 1 and I if the control qubit is 0. (b) Realizing the evolution $\exp(-i\theta P/2)$ itself (with $R_x(\theta) = \exp(-i\theta X/2)$. (c) Realization of circuit (a) using CNOTS when $P = X_1X_2X_3X_4$. (d) Realization of circuit (a) using CNOTs when $P = Z_1Z_2Z_2Z_4$.

The 3-qubit repetition code does not protect or detect Z (dephasing) errors as the parity checks only measure information in the Z-basis (M_Z). Shor's 9-qubit code was the first quantum error-correcting code which encodes a single qubit and corrects any single qubit Pauli error. Shor's code is obtained from the 3-qubit repetition code by *concatenation*. Code concatenation is a procedure in which we take the elementary qubits of the codewords of a code C and replace them by encoded qubits of a new code C'. In Shor's construction we choose the first code C as the repetition code in the Hadamard-rotated basis ($H : X \leftrightarrow Z$) with codewords $|\overline{+}\rangle = |+++\rangle$ and $|\overline{-}\rangle = |---\rangle$. The parity checks of C are X_1X_2 and X_2X_3 and the logical operators are $\overline{Z}_C = Z_1Z_2Z_3$ and $\overline{X}_C = X_1$. As the second code C' we choose the normal 3-qubit repetition code, i.e. we replace $|+\rangle$ by $|\overline{+}\rangle = \frac{1}{\sqrt{2}}(|000\rangle + |111\rangle)$ etc.

We get all the parity checks for the concatenated 9-qubit code by taking all the parity checks of the codes C' and the C'-encoded parity checks of C. For Shor's code this will give: the Z-checks Z_1Z_2, Z_2Z_3, Z_4Z_5, Z_5Z_6, Z_7Z_8 and Z_8Z_9 (from three uses of the code C') and the X-checks $X_1X_2X_3X_4X_5X_6$, $X_4X_5X_6X_7X_8X_9$ (from the parity checks $\overline{X}_1\overline{X}_2$ and $\overline{X}_2\overline{X}_3$ where $\overline{X}$ is the logical operator of the code C'). The non-unique logical operators of the encoded qubit are $\overline{Z} = Z_1Z_4Z_7$ and $\overline{X} = X_1X_2X_3$.

This code can clearly correct any X error as it consists of three qubits each of which is encoded in the repetition code which can correct an X error. What happens if a single Z error occurs on any of the qubits? A single Z error will anti-commute with one of the parity X-checks or with both. For example, the error Z_1 anti-commutes with $X_1X_2X_3X_4X_5X_6$ so that the state $Z_1|\overline{\psi}\rangle$ has eigenvalue -1 with respect to this parity check. The eigenvalues of the parity check operators are called the *error syndrome*. Aside from detecting errors (finding -1 syndrome values) the error syndrome should allow one to infer which error occurred.

One feature of quantum error correcting codes which is different from classical error correcting codes, is that this inference step does not necessarily have to point to a unique error. For example: for the 9-qubit code, the error Z_1 and the error Z_2 have an equivalent effect on the codespace as Z_1Z_2 is a parity check which acts trivially on the code space. The syndromes for errors which are related by parity checks are always identical. The classical algorithm which processes the syndrome to infer an error, —this procedure is called *decoding*—, does not need to choose between such equivalent errors. But there is further ambiguity in the error syndrome. For Shor's code the error Z_1 and the error Z_4Z_7 have an identical syndrome as $Z_1Z_4Z_7$ is the $\overline{Z}$ operator which commutes with all parity checks. If we get a single non-trivial (-1) syndrome for the parity check $X_1X_2X_3X_4X_5X_6$ we could decide that the error is Z_1 or Z_4Z_7. But if we make a mistake in this decision and correct with Z_4Z_7 while Z_1 happened then we have effectively performed a $\overline{Z}$ without knowing it! This means that the decoding procedure

should decide between errors, —all consistent with the error syndrome—, which are mutually related by logical operators.

How is this decision made? We could assign a probability to each possible error: this assignment is captured by the *error model*. Then our decoding procedure can simply choose an error (or class of equivalent errors), consistent with the syndrome, which has highest probability. We will discuss the procedure of decoding more formally in Section II.A.1 after we introduce the stabilizer formalism. For Shor's code we decode the syndrome by picking a single qubit error which is consistent with the syndrome. If a two-qubit error occurred we may thus have made a mistake. However, for Shor's code there are no two single-qubit errors E_1 and E_2 with the same syndrome whose product E_1E_2 is a logical operator. This implies that Shor's code can correct any single qubit error. It is a $[[n,k,d]] = [[9,1,3]]$ code, encoding $k = 1$ qubit into $n = 9$ (n is called the *block size* of the code) and having *distance* $d = 3$. The distance d of the code is defined as the minimum weight of any logical operator (see the formal definition in Eq. (1)). The weight of a Pauli operator is the number of qubits on which it acts non-trivially. We take the minimum weight as there are several logical operators and the weight of each one of them can be varied by multiplication with parity checks. It is simple to understand why a code with distance $d = 2t + 1$ can correct t errors: errors of weight at most t have the property that their products have weight at most $2t < d$ and therefore the product can never be a logical operator as those have weight d or more. Thus our decoding procedure which picks an error of weight at most t can never lead to a logical error. If errors only take place on some *known* subset of qubits, then a code with distance d can correct (errors on) subsets of size $d-1$ as the product of any two Pauli errors on this subset has weight at most $d-1$. In other words, if $d-1$ or fewer qubits of the codeword fall into a black hole (or those qubits are lost or *erased* by other means) one can still recover the entire codeword from the remaining qubits. One could do this by replacing the lost $d-1$ qubits by the completely-mixed state $I/2^{d-1}$ [2], measuring the parity checks on all qubits, determining a lowest-weight Pauli error of weight at most $d-1$ and applying this correction to the $d-1$ qubits.

Clearly, the usefulness of (quantum) error correction is directly related to the error model; it hinges on the assumption that low-weight errors are more likely than high-weight errors. Error-correcting a code which can perfectly correct errors with weight at most t, will lead to failure with probability roughly equal to the total probability of errors of weight larger than t. This probability for failure of error correction is called the *logical error rate*. The goal of quantum error correction is to use redundancy and correction to realize logical qubits with logical error rates below the error rate of the elementary constituent qubits.

It seems rather simplistic to use error models which assign X, Z and Y errors probabilistically to qubits since in real quantum information, amplitudes and phases are evolving continuously in time rather than undergoing discretized errors. Ideal parity measurement can induce such discrete error model stated in terms of probabilities, but as parity measurements themselves will be inaccurate in a continuous fashion, such a fully digitized picture is an oversimplification. The theory of quantum fault-tolerance, see Section II.D, has developed a framework which allows one to establish the results of quantum error correction and fault-tolerance for very general quantum dynamics obeying physical locality assumptions (see the comprehensive results in (Aliferis *et al.*, 2006)). However, for numerical studies of code performance it is impossible to simulate such more general open system dynamics and several simple error models are used to capture the expected performance of the codes.

Three important remarks can be made with this general framework in mind. The simplest message is that 1) a code which can correct t Pauli errors can in fact correct any possible error on a subset of t qubits (described for example by some noisy superoperator or master equation for the qubits), see Section II.B. This point can be readily understood in the case of ideal parity check measurements where the measurement projects the set of possible errors onto the set of Pauli errors. Secondly, 2) errors can be correlated in space and time arising from non-Markovian dynamics, but as long as (1) we use the proper estimate of the strength of the noise (which may involve using amplitudes and norms rather than probabilities) and (2) the noise is sufficiently short-ranged (meaning that noisy interactions between distant uncoupled qubits are sufficiently weak (Aharonov *et al.*, 2006)), fault-tolerance threshold results can be established. The third remark 3) is that qubit coding does not directly deal with leakage errors. As many elementary qubits are realized as two-level subspaces of higher-dimensional systems to which they can leak, other protective mechanisms such as cooling (or teleporting to a fresh qubit) will need to be employed in order to convert a leakage error into a regular error which can be corrected.

Let us come back to Shor's code and imagine that the nine qubits are laid out in a 3×3 square array as in Fig. 2. It looks relatively simple to measure the parity Z-checks locally, while the weight-6 X-checks would require a larger circuit. But why should there be such asymmetry between the X- and Z-checks? Imagine that

[2] The erasure of a qubit, i.e. the qubit state ρ is replaced by $I/2$, can be written as the process of applying a I, X, Y resp. Z error with probability 1/4: $I/2 = (\rho + X\rho X + Z\rho Z + Y\rho Y)/4$.

instead of measuring the 'double row' stabilizer operator $\mathbf{X}_{=,1} \equiv X_1X_2X_3X_4X_5X_6$, we measure (in parallel or sequentially) the eigenvalues of X_1X_4, X_2X_5 and X_3X_6 and take the product of these eigenvalues to obtain the eigenvalue of $\mathbf{X}_{=,1}$. The important property of these weight-2 operators is that they all individually commute with the logical operators $\overline{X}$ and $\overline{Z}$ of the Shor code, hence measuring them does not change the expectation values of $\overline{X}$ and $\overline{Z}$. These weight-2 X-checks do not commute with the weight-2 Z-checks however. If we first measure all the weight-2 X-checks and then measure the Z-checks, then with the second step the eigenvalues of individual X-checks are randomized but correlated. Namely, their product $X_1X_2X_3X_4X_5X_6$ remains fixed as $X_1X_2X_3X_4X_5X_6$ commutes with the weight-2 Z-checks. By symmetry, the weight-2 X-checks commute with the double column operators $\mathbf{Z}_{||,1} = Z_1Z_2Z_4Z_5Z_7Z_8$ and $\mathbf{Z}_{||,2} = Z_2Z_3Z_5Z_6Z_8Z_9$. Viewing the Shor code this way we can imagine doing error correction and decoding using the stable commuting parity checks $\mathbf{X}_{=,1}, \mathbf{X}_{=,2}, \mathbf{Z}_{||,1}, \mathbf{Z}_{||,2}$ while we deduce their eigenvalues from measuring 12 weight-2 parity checks. Shor's code in this form is the smallest member in the family of Bacon-Shor codes $[[n^2, 1, n]]$ (Aliferis and Cross, 2007; Bacon, 2006) whose qubits can be laid out in a $n \times n$ array as in Fig. 14, see Section III.B. The Bacon-Shor code family in which non-commuting (low-weight) parity checks are measured in order to deduce the eigenvalues of commuting parity checks is an example of a (stabilizer) subsystem code.

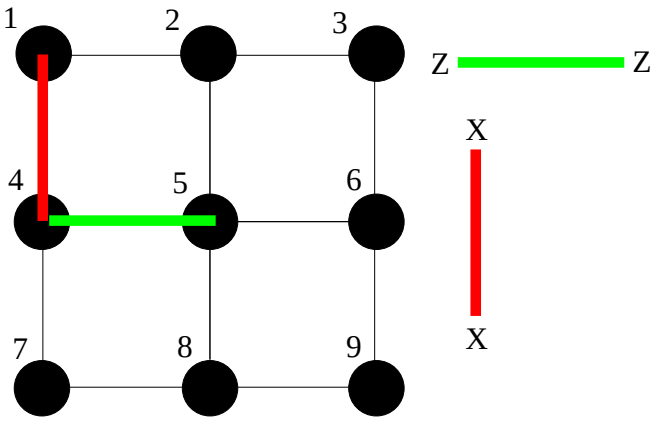

FIG. 2 The 9-qubit $[[9, 1, 3]]$ Shor code with black qubits on the vertices. The stabilizer of Shor's code is generated by the weight-2 Z-checks as well as two weight-6, double row, X-checks $\mathbf{X}_{=,1} = X_1X_2X_3X_4X_5X_6$ and $\mathbf{X}_{=,2}$. An alternative way of measuring $\mathbf{X}_{=,1}$ and $\mathbf{X}_{=,2}$ is by measuring the weight-2 X-checks in the Figure. One can similarly define two weight-6, double column, Z-checks, $\mathbf{Z}_{||,1}$ and $\mathbf{Z}_{||,2}$ as products of elementary weight-2 Z checks. See also Fig. 14.

1. Stabilizer (Subsystem) Codes[3]

Shor's code and many existing codes defined on qubits are examples of *stabilizer* codes (Gottesman, 1997). Stabilizer codes are attractive as (i) they are the straightforward quantum generalization of classical binary linear codes, (ii) their logical operators and distance are easily determined, it is relatively simple to (iii) understand how to construct universal sets of logical gates and (iv) execute a numerical analysis of the code performance. The main idea of stabilizer codes is to encode k logical qubits into n physical qubits using a subspace, the codespace, $\mathcal{L} \subseteq (\mathbb{C}^2)^{\otimes n}$ spanned by states $|\psi\rangle$ that are invariant under the action of a *stabilizer group* $\mathcal{S}$,

$$\mathcal{L} = \{|\psi\rangle \in (\mathbb{C}^2)^{\otimes n} \,:\, P\,|\psi\rangle = |\psi\rangle \quad \forall P \in \mathcal{S}\}.$$

Here $\mathcal{S}$ is an Abelian subgroup of the Pauli group $\mathcal{P}_n = \langle iI, X_1, Z_1, \ldots, X_n, Z_n\rangle$ such that $-I \notin \mathcal{S}$. For any stabilizer group $\mathcal{S}$ one can always choose a set of generators $S_1, \ldots, S_m$, i.e. $\mathcal{S} = \langle S_1, \ldots, S_m\rangle$, such that $S_a \in \mathcal{P}_n$ are hermitian Pauli operators. The mutually commuting parity checks which we considered before are the generators of the stabilizer group. If there are $n-k$ linearly independent generators (parity checks) then the codespace $\mathcal{L}$ is 2^k-dimensional, or encodes k qubits. The *weight* $|P|$ of a Pauli operator $P = P_1 \ldots P_n \in \mathcal{P}_n$ is the number of non-identity single-qubit Pauli operators P_i. If the code encodes k logical qubits, it is always possible to find k pairs of logical operators $(\overline{X}_j, \overline{Z}_j)_{j=1,\ldots,k}$. These logical operators commute with all the parity checks, i.e. they commute with all elements in $\mathcal{S}$ as they preserve the codespace. However they should not be generated by the parity checks themselves otherwise their action on the code space is trivial. The centralizer $\mathcal{C}(\mathcal{S})$ of $\mathcal{S}$ in $\mathcal{P}_n$ is defined as $\mathcal{C}(\mathcal{S}) = \{P \in \mathcal{P}_n | \forall s \in \mathcal{S},\ Ps = sP\}$, i.e. all operators in $\mathcal{P}_n$ which commute with $\mathcal{S}$. We thus have $\mathcal{C}(\mathcal{S}) = \langle \mathcal{S}, \overline{X}_1, \overline{Z}_1, \ldots, \overline{X}_k, \overline{Z}_k\rangle$, i.e. the logical operators of the code are elements of $\mathcal{C}(\mathcal{S}) \setminus \mathcal{S}$ as they are in $\mathcal{C}(\mathcal{S})$ but not in $\mathcal{S}$. The distance d of a stabilizer code can then be defined as

$$d = \min_{P \in \mathcal{C}(\mathcal{S}) \setminus \mathcal{S}} |P|. \tag{1}$$

Error correction proceeds by measuring the error syndrome $\mathbf{s}$ which are the ± 1 eigenvalues of the generators of $\mathcal{S}$. As we mentioned in Section II.A this syndrome will not point to a unique Pauli error but an *equivalence class of errors*, namely all $E' = EP$ where $P \in \mathcal{C}(\mathcal{S})$ give rise to the same syndrome. We can define an error coset $E\mathcal{S} = [E]$ of the group $\mathcal{S}$ in $\mathcal{P}_n$ [4], consisting of errors $E' = EP$ where $P \in \mathcal{S}$, that is, elements in $[E]$ are

[3] Readers less interested in this general framework can skip this section without major inconvenience.

[4] Note that left and right cosets are the same modulo trivial errors proportional to I.

related to E by a (trivially-acting) element in the stabilizer group. We can associate a total error probability with such coset, $\text{Prob}([E]) = \sum_{s\in S} \text{Prob}(Es)$, depending on some error model which assigns a probability $\text{Prob}(P)$ to every Pauli operator $P \in \mathcal{P}_n$. Given an error E and a syndrome, one can similarly define a discrete number of cosets $[E\overline{P}]$ where the logicals $\overline{P} \in \mathcal{C}(\mathcal{S})\backslash\mathcal{S}$. *Maximum likelihood* decoding is the procedure by which, given a syndrome $\mathbf{s}$ and a coset representative $E(\mathbf{s})$, one finds the logical operator $\overline{P}$ (which could be I) which has the maximum value for $\text{Prob}([E\overline{P}])$. If we take the coset representative $E(\mathbf{s})$ to be the error E which actually took place, then such decoding is successful when $\text{Prob}([E])$ is larger than $\text{Prob}([E\overline{P}])$ for any non-trivial $\overline{P}$.

It is important to consider how efficiently (in the number n of elementary qubits) maximum likelihood decoding can be done since $\text{Prob}([E\overline{P}])$ is a sum over the number of elements in $\mathcal{S}$ which is exponential in n. For a simple depolarizing error model where each qubit undergoes a X, Y or Z error with probability $p/3$ and no error with probability $1-p$, we have $\text{Prob}([E\overline{P}]) = (1-p)^n \sum_{s\in\mathcal{S}} \exp(-\beta|E\overline{P}s|)$ with inverse 'temperature' $\beta = \ln(3(1-p)/p)$. For small error rates $p \ll 1$ corresponding to low temperatures $\beta \to \infty$, the value of this 'partition function' is dominated by the contribution of the lowest-weight error(s). Such lowest-weight error corresponds to a minimum of the energy function $H_E(s) \equiv |Es|$. Thus, instead of maximum likelihood decoding which compares the relative values of $\text{Prob}([E\overline{P}])$, one can also opt for *minimum-weight* decoding. In minimum-weight decoding one simply picks an error $E(\mathbf{s})$, consistent with the syndrome $\mathbf{s}$, which has minimum weight $|E|$. We will discuss this decoding method for the surface code in Section III. For topological codes, the criterion for succesful maximum likelihood decoding and the noise threshold of the code can be related to a phase-transition in a classical statistical model with quenched disorder (Dennis *et al.*, 2002), (Katzgraber and Andrist, 2013).

Subsystem stabilizer codes can be viewed as stabilizer codes in which some logical qubits, called gauge qubits, are not used to encode information (Poulin, 2005). The state of these qubits is irrelevant and can be fixed (gauge-fixing) or left variable. The presence of the gauge qubits sometimes lets one simplify the measurement of the stabilizer parity checks as the state of the gauge qubits is allowed to freely change under these measurements. One takes a stabilizer code $\mathcal{S}$ and splits its logical operators $(\overline{X}_i, \overline{Z}_i)$ into two groups: the gauge qubit logical operators $(\overline{X}_i, \overline{Z}_i)$, $i = 1 \dots m$ and the remaining logical operators $(\overline{X}_i, \overline{Z}_i)$ with $i = m+1, \dots k$. We define a new subgroup $\mathcal{G} = \langle \mathcal{S}, \overline{X}_1, \overline{Z}_1, \dots \overline{X}_m, \overline{Z}_m \rangle$ which is non-Abelian and contains $\mathcal{S}$. As $\mathcal{G}$ is non-Abelian we can consider its center, i.e. $\mathcal{G} \cap \mathcal{C}(\mathcal{G}) = \{P \in \mathcal{G} |\ \forall g \in \mathcal{G}, Pg = gP\} = \mathcal{S}$ (modulo trivial elements).

If we measure the generators of the group $\mathcal{G}$ we can deduce the eigenvalues of $\mathcal{S}$. Since the $k-m$ logical operators $(\overline{X}_i, \overline{Z}_i)$, $i = m+1, \dots, k$ commute with $\mathcal{G}$, these logical operators are unaffected by the measurement. A priori, there is no reason why measuring the generators of $\mathcal{G}$ would be simpler than measuring the generators of the stabilizer $\mathcal{S}$. In the interesting constructions such as the Bacon-Shor code and the subsystem surface code discussed in Section III, we gain because we measure very low-weight parity checks in $\mathcal{G}$ (while we lose by allowing more qubit-overhead or declining noise threshold).

The distance of a subsystem code is not the same as that of a stabilizer code, Eq. (1), as we should only consider the minimum weight of the $k-m$ logical operators. These logical operators are not unique as they can be multiplied by elements in $\mathcal{S}$ *but also* by the logical operators of the irrelevant gauge qubits. This motivates the definition of the distance as $d = \min_{P\in\mathcal{C}(\mathcal{S})\backslash\mathcal{G}} |P|$. As errors on the gauge qubits are harmless it means that equivalent classes of errors are those related to each other by elements in $\mathcal{G}$. Given the eigenvalues of the stabilizer generators, the syndrome $\mathbf{s}$, the decoding algorithm considers cosets $E(\mathbf{s})\mathcal{G}$ in $\mathcal{P}_n$, denoted as $[E] = E\mathcal{G}$. Maximum likelihood decoding proceeds by determining the coset $[E\overline{P}]$ which has a maximum value for $\text{Prob}([E\overline{P}]) = \sum_{g\in\mathcal{G}} \text{Prob}(E\overline{P}g)$ where $\overline{P}$ varies over the possible logical operators.

2. Stabilizer Code Examples and The CSS Construction

We discuss a few small examples of stabilizer codes to illustrate the formalism. For the two-qubit code with $|\overline{0}\rangle = \frac{1}{\sqrt{2}}(|00\rangle + |11\rangle)$ and $|\overline{1}\rangle = \frac{1}{\sqrt{2}}(|01\rangle + |10\rangle)$ we have $\overline{X} = X_1$ or $\overline{X} = X_2$ and $\overline{Z} = Z_1Z_2$. The code can detect any single Z error as such error maps the two codewords onto the orthogonal states $\frac{1}{\sqrt{2}}(|00\rangle - |11\rangle)$ and $\frac{1}{\sqrt{2}}(|01\rangle - |10\rangle)$ (as $\overline{Z}$ is of weight-2). The code can't detect single X errors as these are logical operators.

The smallest non-trivial quantum code is the $[[4, 2, 2]]$ error-detecting code. Its linearly independent parity checks are $X_1X_2X_3X_4$ and $Z_1Z_2Z_3Z_4$: the code encodes $4-2 = 2$ qubits. You can verify that you can choose $\overline{X}_1 = X_1X_2, \overline{Z}_1 = Z_1Z_3$ and $\overline{X}_2 = X_2X_4$, $\overline{Z}_2 = Z_3Z_4$ as the logical operators which commute with the parity checks. The code distance is 2 which means that the code cannot correct a single qubit error. The code can however still *detect* any single qubit error as any single qubit error anti-commutes with at least one of the parity checks which leads to a nontrivial -1 syndrome. Alternatively, we can view this code as a subsystem code which has one logical qubit, say, qubit 1, and one gauge qubit, qubit 2. In that case $\mathcal{G} = \langle X_1X_2X_3X_4, Z_1Z_2Z_3Z_4, Z_3Z_4, X_2X_4\rangle = \langle Z_1Z_2, Z_3Z_4, X_1X_3, X_2X_4\rangle$, showing that measuring weight-2 checks would suffice to detect single qubit errors on the encoded qubit 1. The smallest stabilizer

code which encodes 1 qubit and corrects 1 error is the $[[5,1,3]]$ code; you can find its parity checks in (Nielsen and Chuang, 2000).

Another example is the stabilizer code C_6 (defined in (Knill, 2005)) with parity checks $X_1X_4X_5X_6$, $X_1X_2X_3X_6$, $Z_1Z_4Z_5Z_6$ and $Z_1Z_2Z_3Z_6$ acting on 6 qubits. This code has 4 independent parity checks, hence it encodes $6-4=2$ qubits with the logical operators $\overline{X}_1 = X_2X_3$, $\overline{Z}_1 = Z_1Z_2Z_4$ and $\overline{X}_2 = X_1X_2X_4$, $\overline{Z}_2 = Z_4Z_5$. As its distance is 2, it can only detect single X or Z errors (but note that it can correct a single X error on qubit 1, or Z error on qubit 2).

One can concatenate this code C_6 with the code $[[4,2,2]]$ (called C_4 in (Knill, 2005)) by replacing the three pairs of qubits, i.e. the pairs (12), (34) and (56), in C_6 by three sets of C_4-encoded qubits, to obtain a new code. This code has thus $n=12$ qubits and encodes $k=2$ qubits. We can represent these 12 qubits as 3 sets of 4 qubits such that the X-checks read

$$\mathcal{S}(X) = \left(\begin{array}{cccc|cccc|cccc} X&X&X&X&I&I&I&I&I&I&I&I\\ I&I&I&I&X&X&X&X&I&I&I&I\\ I&I&I&I&I&I&I&I&X&X&X&X\\ X&X&I&I&I&X&I&X&X&I&I&X\\ X&I&I&X&X&X&I&I&I&X&I&X \end{array}\right)$$

The Z-checks are

$$\mathcal{S}(Z) = \left(\begin{array}{cccc|cccc|cccc} Z&Z&Z&Z&I&I&I&I&I&I&I&I\\ I&I&I&I&Z&Z&Z&Z&I&I&I&I\\ I&I&I&I&I&I&I&I&Z&Z&Z&Z\\ Z&I&Z&I&I&I&Z&Z&Z&I&I&Z\\ Z&I&I&Z&Z&I&Z&I&I&I&Z&Z \end{array}\right).$$

and the logical operators are

$$\begin{array}{cccc|cccc|cccc} \overline{X}_1 = & I&X&I&X&X&X&I&I&I&I&I&I\\ \overline{Z}_1 = & Z&I&I&Z&I&I&Z&Z&I&I&I&I\\ \overline{X}_2 = & X&I&I&X&I&X&I&X&I&I&I&I\\ \overline{Z}_2 = & I&I&I&I&I&I&Z&Z&Z&I&Z&I \end{array}$$

One can verify that the minimum weight of the logical operators of this concatenated code is 4. Thus the code is a $[[12,2,4]]$ code, able to correct any single error and to detect any three errors.

One could repeat the concatenation step and recursively concatenate C_6 with itself (replacing a pair of qubits by three pairs of qubits etc.) as in Knill's C_4/C_6 architecture (Knill, 2005) or, alternatively, recursively concatenate C_4 with itself as was considered in (Aliferis and Preskill, 2009). Note that in general when we concatenate a $[[n_1,1,d_1]]$ code with a $[[n_2,1,d_2]]$ code, we obtain a code which encodes one qubit into $n=n_1n_2$ qubits and has distance $d=d_1d_2$. Code concatenation is a useful way to obtain a large code from smaller codes as the number of syndrome collections scales linearly with the number of concatenation steps while the number of qubits and the distance grows exponentially with the number of concatenation steps. In addition, decoding of a concatenated code is efficient in the block-size n of the code and the performance of decoding can be strongly enhanced by using message passing between concatenation layers (Poulin, 2006).

Another well-known code is Steane's 7-qubit code, $[[7,1,3]]$ which is constructed from two classical codes using the Calderbank-Shor-Steane (CSS) construction (Nielsen and Chuang, 2000). Classical binary linear codes are fully characterized by their parity check matrix H. The parity check matrix H_1 of a code C_1 encoding k_1 bits is a $(n-k_1)\times n$ matrix with 0,1 entries where linearly independent rows represent the parity checks. The binary vectors $c\in\{0,1\}^n$ which obey the parity checks, i.e. $Hc=0$ (where addition is modulo 2), are the codewords. The distance $d=2t+1$ of such classical code is the minimum (Hamming) weight of any codeword and the code can correct t errors. We can represent a row r of H_1 of a code C_1 by a parity check operator $s(Z)$ such that for the bit $r_i=1$ we take $s(Z)_i=Z$ and for bit $r_i=0$ we set $s(Z)_i=I$. These parity checks generate some stabilizer group $\mathcal{S}_1(Z)$. In order to make this into a quantum code with distance larger than one, one needs to add X-type parity checks. These could simply be obtained from the $(n-k_2)\times n$ parity check matrix H_2 of another classical code C_2. We obtain the stabilizer parity checks $\mathcal{S}_2(X)$ by replacing the 1s in each row of this matrix by Pauli X and I otherwise. But in order for $\mathcal{S}=\langle\mathcal{S}_1(Z),\mathcal{S}_2(X)\rangle$ to be an Abelian group the checks all have to commute. This implies that every parity X-check should overlap on an even number of qubits with every parity Z-check. In coding words it means that the rows of H_2 have to be orthogonal to the rows of H_1. This in turn can be expressed as $C_2^\perp\subseteq C_1$ where $C_2^\perp$ is the code dual to C_2 (codewords of $C_2^\perp$ are all the binary vectors orthogonal to all codewords $c\in C_2$).

In total $\mathcal{S}=\langle\mathcal{S}_1(Z),\mathcal{S}_2(X)\rangle$ will be generated by $2n-k_1-k_2$ independent parity checks so that the quantum code encodes k_1+k_2-n qubits. The distance of the quantum code is the minimum of the distance $d(C_1)$ and $d(C_2)$ as one code is used to correct Z errors and the other code is used to correct X errors.

A good example is Steane's code which is constructed using a classical binary code C which encodes 4 bits into 7 bits and has distance 3. Its parity check matrix is

$$H = \left(\begin{array}{ccccccc} 0&0&0&1&1&1&1\\ 0&1&1&0&0&1&1\\ 1&0&1&0&1&0&1 \end{array}\right). \qquad (2)$$

The codewords c which obey $Hc=0$ are linear combinations of the $7-3=4$ binary vectors $(1,1,1,0,0,0,0)$, $(0,0,0,1,1,1,1)$, $(0,1,1,0,0,1,1)$, $(1,0,1,0,1,0,1)$ where the last three are the rows of the parity check matrix: these are also codewords of $C^\perp$. Hence $C^\perp\subseteq C$ and we can use the CSS construction

with $C_1 = C$ and $C_2 = C$ to get a quantum code. As $C^\perp$ (as well as C) has distance 3, the quantum code will have distance 3 and encodes one qubit. The parity checks are $Z_4Z_5Z_6Z_7$, $Z_2Z_3Z_6Z_7$, $Z_1Z_3Z_5Z_7$ and $X_4X_5X_6X_7$, $X_2X_3X_6X_7$, $X_1X_3X_5X_7$.

B. QEC Conditions and Other Small Codes of Physical Interest

One may ask what properties a general (not necessarily stabilizer) quantum code, —defined as some subspace C of a physical state space—, should obey in order for a certain set of errors to be correctable. These properties are expressed as the quantum error-correcting conditions which can hold exactly or only approximately. We encode some k qubits into a codespace C so that $|\bar{i}\rangle$ are the codewords encoding the k-bit strings i. Assume there is a set of errors $\mathcal{E} = \{E_l\}$ against which we wish to correct. The quantum error-correcting conditions (Nielsen and Chuang, 2000) say that there exists an error-correcting operation, a reversal of the error, if and only if the following conditions are obeyed for all errors $E_k, E_l \in \mathcal{E}$

$$\forall i,j\ , \langle \bar{i}|E_k^\dagger E_l|\bar{j}\rangle = c_{kl}\delta_{ij}. \tag{3}$$

Here c_{kl} is a constant *independent* of the codeword $|\bar{i}\rangle$ with $c_{kl} = c_{lk}^*$. The condition for $i = j$ informally says that the codewords are not distinguished by the error observables. The condition for $i \neq j$ indicates that the orthogonal codewords need to remain orthogonal after the action of the errors (otherwise we could not undo the effect of the noise). One can find a derivation of these conditions in (Nielsen and Chuang, 2000). If a code can correct the error set $\{E_i\}$ it can also correct an error set $\{F_j\}$ where each F_j is any linear combination of the elements E_i as one can verify that the set $\{F_j\}$ will also obey the quantum error-correcting conditions of Eq. (3). This means that if a code can correct against Pauli errors on any subset of k qubits, it can correct against any error on k qubits as the Pauli matrices form an operator basis in which one can expand the errors.

These QEC conditions can be generalized to the unified framework of operator quantum error correction (Kribs *et al.*, 2005; Nielsen and Poulin, 2007) which covers both subsystem codes as well as error-avoidance techniques via the use of decoherence-free subspaces and noise-free subsystems.

How do we determine the set of error operators $\{E_i\}$ for a given set of qubits? In principle, one could start with a Hamiltonian description of the dynamics of the qubits, the system S, coupled to a physically-relevant part of the rest of the world, which we call the environment E. In other wards, one has a Hamiltonian $H(t) = H_S(t) + H_{SE}(t) + H_E(t)$ where $H_{SE}(t)$ is the coupling term. We assume that the qubits of the system and environment are initially ($t = 0$) in some product state $\rho_S \otimes \rho_E$ and then evolve together for time τ. The dynamics due to the $U(0,\tau) = \mathcal{T}\exp(-i\int_0^\tau dt' H(t'))$, for the system alone can then be described by the superoperator $\mathcal{S}_\tau$:

$$\mathcal{S}_\tau(\rho_S) = \mathrm{Tr}_E\, U(0,\tau)\rho_S\otimes\rho_E U^\dagger(0,\tau) = \sum_i E_i\rho_S E_i^\dagger,$$

where we can identify $\{E_i\}$ with $\sum_i E_i^\dagger E_i = I$ as the Kraus error operators. This derivation of the error operators is appropriate when the system-environment interaction is memory-less or Markovian beyond a timescale τ. For general non-Markovian noise such description is not appropriate and could be replaced by an expansion of the joint unitary transformation $U(t_1,t_2) = U_{ideal}(t_1,t_2) + E_{SE}$ with $U_{ideal}(t_1,t_2)$ is the ideal faultless evolution. The operator E_{SE} can always be expanded as $E_{SE} = \sum_i E_i \otimes B_i$ where $\{E_i\}$ can be identified as a set of error operators on the system. We refer to the book (Lidar and Brun, 2013) for a more extensive treatment of non-Markovian noise models.

Quite commonly one can describe the open system dynamics by a Markovian master equation of the Lindblad form

$$\frac{d\rho}{dt} = -i[H(t),\rho] + \mathcal{L}(\rho) \equiv \mathcal{L}_{\mathrm{tot}}(\rho) \tag{4}$$

where $\mathcal{L}(\rho) = \sum_j L_j\rho L_j^\dagger - \frac{1}{2}\{L_j^\dagger L_j,\rho\}$ with quantum-jump or Lindblad operators L_j. Here $H(t)$ is the Hamiltonian of the quantum system which could include some time-dependent drives. For short times τ we have $\rho(\tau) = \mathcal{S}_\tau(\rho(0)) = E_0\rho E_0^\dagger + \sum_i E_i\rho E_i^\dagger$ with $E_0 \approx I - i\tau H - \frac{1}{2}\tau\sum_i L_i^\dagger L_i = I - O(\tau)$ and $E_i \approx \sqrt{\tau}L_i$. Thus the error set is given by the quantum jump operators L_i and the no-error operator E_0 which is nontrivial in order $O(\tau)$.

A special simple case of such Lindblad equation leads to the Bloch equation which is used to describe qubit decoherence at a phenomenological level. We consider a qubit, described by a Hamiltonian $H = -\frac{\omega}{2}Z$, which exchanges energy with a large Markovian environment in thermal equilbrium at temperature $\beta = \frac{1}{kT}$. One can model such open-system dynamics using a Davies master equation of Lindblad form with quantum jump operators with $L_- = \sqrt{\kappa_-}\sigma_-$ and $L_+ = \sqrt{\kappa_+}\sigma_+$ where the rates κ_+, κ_- obey a detailed balance condition $\frac{\kappa_+}{\kappa_-} = \exp(-\beta\omega)$. The resulting Lindblad equation has the thermal state $\rho_\beta = \frac{\exp(-\beta H)}{\mathrm{Tr}(\exp(-\beta H))}$ as its unique stationary point for which $\mathcal{L}_{tot}(\rho_\beta) = 0$. We can include additional physical sources of qubit dephasing modeled by quantum jump operator $L_Z = \sqrt{\gamma_Z}Z$ in the Lindblad equation; this, of course, does not alter its stationary point.

We can parametrize a qubit as $\rho = \frac{1}{2}(I + \mathbf{r}\cdot\sigma)$ with Bloch vector $\mathbf{r}$ and Pauli matrices $\sigma = (X,Y,Z)$ and re-express such Lindblad equation as a differential equation

for $\mathbf{r}$, the Bloch equation. Aside from the process of thermal equilibration and dephasing, one may add time-dependent driving fields in the Bloch equation (which are assumed not to alter the equilibration process) so that the general Hamiltonian is $H(t) = \frac{1}{2}\mathbf{M}(t) \cdot \sigma$.

The Bloch equation then reads

$$\frac{d\mathbf{r}}{dt} = \mathbf{r}(t) \times \mathbf{M}(t) + \mathbf{R}(\mathbf{r}(t) - \mathbf{r}_\beta), \tag{5}$$

where the first (second) part describes the coherent (dissipative) dynamics. Here the equilibrium Bloch vector $\mathbf{r}_\beta = (0, 0, \tanh(\beta\omega/2))$ and the diagonal relaxation matrix equals $\mathbf{R} = \mathrm{diag}(-1/T_2, -1/T_2, -1/T_1)$ where the decoherence time T_2 and relaxation time T_1 characterize the basic quality of the qubit.

We will consider two simple codes which approximately obey the conditions in Eq. (3) for physically relevant (amplitude) damping for qubits and bosonic modes. Even though the $[[5, 1, 3]]$ code is the smallest code which can correct against any single qubit error, one can use 4 qubits to approximately correct any *amplitude-damping* error which can model energy loss (Leung *et al.*, 1997). The noise process for amplitude damping on a single qubit is given by the superoperator $\mathcal{S}(\rho) = \sum_i A_i \rho A_i^\dagger$ with $A_0 = \frac{1}{2}((1+\sqrt{1-\kappa})I + (1-\sqrt{1-\kappa})Z) \approx I - O(\kappa)$ and $A_1 = \sqrt{\kappa}\sigma_-$ with $\sigma_- = |0\rangle\langle 1|$. The codewords for the 4-qubit amplitude damping code are $\left|\overline{0}\right\rangle = \frac{1}{\sqrt{2}}(|0000\rangle + |1111\rangle)$ and $\left|\overline{1}\right\rangle = \frac{1}{\sqrt{2}}(|0011\rangle + |1100\rangle)$. Each qubit in this code is subjected to amplitude-damping noise. We wish to approximately correct against the error set $E_0 = A_0A_0A_0A_0$, $E_1 = A_1A_0A_0A_0$, $E_2 = A_0A_1A_0A_0, E_3 = A_0A_0A_1A_0, E_4 = A_0A_0A_0A_1$, corresponding to no damping and single qubit damping on any of the four qubits respectively. The authors in (Leung *et al.*, 1997) show that this code obeys the QEC conditions approximately with $O(\kappa^2)$ corrections which is a quadratic improvement over the basic error rate κ. Clearly, when one uses an approximate error correction code, one can only approximately undo the errors. Determining an optimal recovery (defined as optimizing a worst-case or average-case fidelity) is more involved, see e.g. the most recent results on this code and the general approach in (Ng and Mandayam, 2010).

1. Qubit-into-Oscillator Codes

Another interesting example is that of a single bosonic mode (with creation and annihilation operators $a^\dagger, a$) which is used to encode a qubit in two orthogonal states which are approximately protected against photon loss. The damping process can be modeled with the Lindblad equation, Eq. (4), with $L = \sqrt{\kappa}a$ while $H = \omega(a^\dagger a + \frac{1}{2})$ (which we can transform away by going to the rotating frame at frequency ω). One can choose two Schrödinger cat states as encoded states $\left|\overline{0}_+\right\rangle$, $\left|\overline{1}_+\right\rangle$ with

$$\begin{aligned}\left|\overline{0}_\pm\right\rangle &= \frac{1}{\sqrt{N_\pm}}\left(|\alpha\rangle \pm |-\alpha\rangle\right), \\ \left|\overline{1}_\pm\right\rangle &= \frac{1}{\sqrt{N_\pm}}\left(|i\alpha\rangle \pm |-i\alpha\rangle\right).\end{aligned} \tag{6}$$

Here $|\alpha\rangle$ is a coherent state $|\alpha\rangle = \exp(-|\alpha|^2/2)\sum_n \frac{\alpha^n}{\sqrt{n!}}|n\rangle$ and $N_\pm = 2(1 \pm \exp(-2|\alpha|^2)) \approx 2$. For sufficiently large photon number $\langle n\rangle = |\alpha|^2$, the states $|\pm\alpha\rangle, |\pm i\alpha\rangle$, and therefore $\left|\overline{0}_+\right\rangle$ and $\left|\overline{1}_+\right\rangle$, are approximately orthogonal (as $|\langle\alpha|\beta\rangle|^2 = \exp(-|\alpha-\beta|^2)$). The creation and manipulation of cat states has been actively explored, see an extensive discussion on cavity-mode cats in microwave cavities (Haroche and Raimond, 2006). The code states are chosen such that loss of a photon from the cavity maps the states onto (approximately) orthogonal states. As $a|\alpha\rangle = \alpha|\alpha\rangle$, we have

$$a\left|\overline{0}_+\right\rangle = \alpha\sqrt{N_+/N_-}\left|\overline{0}_-\right\rangle,\ a\left|\overline{1}_+\right\rangle = i\alpha\sqrt{N_+/N_-}\left|\overline{1}_-\right\rangle, \tag{7}$$

with $\left|\overline{0}_-\right\rangle, \left|\overline{1}_-\right\rangle$ defined in Eq. (6). The preservation of orthogonality is a prerequisite for these code states to be correctable. More precisely, one can verify that in the limit $|\alpha| \to \infty$ one obeys the QEC conditions[5], Eq. (3), for $E_0 = \sqrt{\kappa}a$ and $E_1 = I - \frac{\kappa}{2}a^\dagger a$. The codespace (spanned by $\left|\overline{0}_+\right\rangle, \left|\overline{1}_+\right\rangle$) is distinguished from the orthogonal erred space (spanned by $\left|\overline{0}_-\right\rangle$ and $\left|\overline{1}_-\right\rangle$) by the photon parity operator $\exp(i\pi a^\dagger a) = \sum_n (-1)^n |n\rangle\langle n| = P_{even} - P_{odd}$. This parity operator has $+1$ eigenvalue for the even photon number states $\left|\overline{0}_+\right\rangle, \left|\overline{1}_+\right\rangle$ and -1 eigenvalue for the odd photon number states $\left|\overline{0}_-\right\rangle, \left|\overline{1}_-\right\rangle$. By continuously monitoring the value of the parity operator one could track the occurrence of errors (Haroche *et al.*, 2007; Sun *et al.*, 2013). Better even would be the realization of a restoring operation which puts back an erred state with decayed amplitude $\alpha e^{-\kappa t/2}$ into the code space while restoring the amplitude back to α. However such restorative process will always add noise to the codewords as it is physically impossible to increase the distinguishability between (decayed) non-orthogonal code words. Thus starting with cat states with finite α, after repeated cycles of errors followed by assumingly perfect error detection and correction, the cat states will gradually loose their intensity and thus their approximate protection. In (Leghtas *et al.*, 2013; Mirrahimi *et al.*, 2013) the interaction of superconducting qubits

[5] If we were to use two coherent states as code states, say, $\left|\overline{0}\right\rangle = |\alpha\rangle$ and $\left|\overline{1}\right\rangle = |-\alpha\rangle$, the QEC conditions would not be obeyed, as $\langle\alpha|E_1^\dagger E_0|\alpha\rangle \neq \langle -\alpha|E_1^\dagger E_0|-\alpha\rangle$ for any α.

coupled to 2D or 3D microwave cavities (circuit QED) is proposed to be used for encoding, correction and decoding of such cat states.

One can generalize the stabilizer formalism to continuous-variable systems characterized by an infinite-dimensional Hilbert space (Braunstein, 1998; Lloyd and Slotine, 1998) (see also (Harrington, 2004)). Of particular interest are codes which encode a discrete amount of information, a qubit say, in a harmonic oscillator (Gottesman *et al.*, 2001). Given are two conjugate variables $\hat{p}$ and $\hat{q}$ which represent generalized momentum and position, obeying $[\hat{q}, \hat{p}] = i$. The idea is to encode the information such that *small* shifts in position or momentum correspond to correctable errors while logical operators are represented as large shifts. For a harmonic oscillator space, the Pauli group P_n can be generalized to the Weyl-Heisenberg group generated by the unitary operators $\exp(it\hat{p})$ and $\exp(is\hat{q})$ for real s and t. In order to define a qubit in this infinite-dimensional space we select a set of commuting check generators whose $+1$ eigenvalue space is two-dimensional.

We will consider two examples. In our first example the codespace is a single state and essentially represents a quantum rotor. We choose $S_q = e^{2i\hat{q}}$ and $S_p = e^{-i\pi\hat{p}}$ as commuting check operators [6]. When $S_p = 1$ and $S_q = 1$ the eigenvalues of $\hat{p}$ are even integers while $\hat{q}$ should have eigenvalues $0 \mod \pi$. Defining $\hat{n} = \hat{p}/2$ and $\hat{\phi} = 2\hat{q}$, we obtain a quantum rotor with conjugate variables $\hat{n} = 0, \pm 1, \ldots$ and 2π-periodic phase $\hat{\phi}$. A realization of the quantum rotor is the quantization of a superconducting circuit where ϕ is the superconducting phase (difference phase across a Josephson junction) and $\hat{n}$ represents the number of Cooper pairs (difference number of Cooper pairs across a Josephson junction). As there is a unique state with fixed (say $+1$) eigenvalues for S_q and S_p, superconducting qubits such as, for example, the transmon qubit (Koch *et al.*, 2007) use superpositions of states with different eigenvalues for $S_q = e^{i\phi}$ in order to encode information. This type of qubit has thus no intrinsic protection against dephasing, i.e. the value of the energy-level splitting is affected by charge and flux noise (representable as linear combinations of small shifts in $\hat{p}$ and $\hat{q}$).

A different choice of S_q and S_p leads to a real code which encodes a single qubit and has built-in protection. We choose as checks the operators $S_q = e^{2i\hat{q}}$ and $S_p = e^{-2i\pi\hat{p}}$. Fixing the eigenvalues of these operators to be $+1$ leads to the discretization $\hat{p} = 0, \pm 1, \pm 2 \ldots$ and again $\hat{q}$ should have eigenvalues which are multiples of π. Now there are two operators which commute with S_q and S_p but which mutually anti-commute: these are $\overline{Z} = e^{i\hat{q}}$ and $\overline{X} = e^{-i\pi\hat{p}}$. One can verify the proper commutation relations of S_q, S_p, $\overline{X}$ and $\overline{Z}$, using $e^A e^B = e^{[A,B]} e^B e^A$ (when A, B are linear combinations of $\hat{q}$ and $\hat{p}$).

The state $\left|\overline{0}\right\rangle$ (defined by $\overline{Z}\left|\overline{0}\right\rangle = \left|\overline{0}\right\rangle$ and $S_p\left|\overline{0}\right\rangle = \left|\overline{0}\right\rangle$) is a uniform superposition of states with $\hat{q} = 0, \pm 2\pi, \ldots$. Similarly, $\left|\overline{1}\right\rangle$ corresponds to a uniform superposition of $\hat{q} = \pm\pi, \pm 3\pi, \ldots$, see Fig. 3 with $\alpha = \pi$. Consider the effect of shifts of the form $e^{i\delta\hat{p}}$ where $|\delta| < \pi/2$, which are correctable. Such shifts map the codewords outside of the codespace as they do not commute with the stabilizer operator S_q. Error correction thus takes place by measuring $q \mod \pi$ and applying the smallest shift which resets $q = 0 \mod \pi$. Similarly, the $|\overline{+}\rangle$ is a uniform superposition of states with $\hat{p} = 0, \pm 2, \pm 4, \ldots$ while $|\overline{-}\rangle$ is a uniform superposition of states with $\hat{p} = \pm 1, \pm 3, \ldots$, see Fig. 3. The qubit is protected against shifts $e^{i\epsilon\hat{q}}$ with $|\epsilon| < 1/2$.

This code space can be viewed as the state space of a Majorana fermion qubit (Alicea, 2012) where $\hat{p} = \hat{n}$ counts the total number of electrons while $\hat{q} = \hat{\phi}$ is the π-periodic conjugate phase variable. The $|\overline{+}\rangle$ eigenstate of $\overline{X}$ with an even number of electrons correspond to the Majorana mode unoccupied while $|\overline{-}\rangle$ is the state with an odd number of electrons as the Majorana mode is occupied. The protection of the Majorana fermion qubit can thus also be understood from this coding perspective although the perspective sheds no light on how to physically realize this qubit or nor the effect of noise which is not represented by these degrees of freedom.

Another representation of this code space, which does not use Majorana fermion qubits, but superconducting circuits is the 0-π qubit (see e.g. (Kitaev, 2006)) which is designed such that the superconducting phase difference between terminals has degenerate energy minima at 0 and π corresponding to the approximate codewords $\left|\overline{0}\right\rangle$ and $\left|\overline{1}\right\rangle$.

More generally, we can parametrize this code by a real number α by taking the stabilizer checks as $S_q = e^{2i\pi\hat{q}/\alpha}$ and $S_p = e^{-2i\hat{p}\alpha}$ (above we took $\alpha = \pi$). The logical operators are $\overline{Z} = e^{\pi i\hat{q}/\alpha}$ and $\overline{X} = e^{-i\hat{p}\alpha}$ (Gottesman *et al.*, 2001), see the codewords in Fig. 3. The code can correct against shifts $e^{i\epsilon\hat{q}}$ with $|\epsilon| < \frac{\pi}{2\alpha}$ and $e^{-i\delta\hat{p}}$ where $|\delta| < \frac{\alpha}{2}$.

One can use this code for encoding a qubit in a bosonic mode where $\hat{q}$ and $\hat{p}$ arise as quadrature variables, i.e. $\hat{q} = \frac{1}{\sqrt{2}}(a^\dagger + a)$ and $\hat{p} = \frac{i}{\sqrt{2}}(a^\dagger - a)$. The free Hamiltonian $H_0 = \omega(a^\dagger a + \frac{1}{2})$ will periodically transform $\hat{q}$ into $\hat{p}$ and vice versa so it is natural to let S_q be of the same form as S_p and choose $\alpha = \sqrt{\pi}$. It can be shown (Gottesman *et al.*, 2001) that errors such as photon loss $L_- = \sqrt{\kappa_-}a$, photon gain $L_+ = \sqrt{\kappa_+}a^\dagger$, dephasing (or decay) of the oscillator $e^{i\theta a^\dagger a}$ (or $e^{-\kappa a^\dagger a}$), or a non-linearity $e^{iK(a^\dagger a)^2}$ for

[6] As $\hat{q}$ and $\hat{p}$ are dimensionful quantities one should take $S_q = e^{2i\hat{q}/q_0}$ and $S_p = e^{-i\pi\hat{p}/p_0}$ where q_0 and p_0 set the scale so that $\hat{q}/q_0$ etc. are dimensionless. In what follows we tacitly assume the existence of such a scale so that if, say, the codespace corresponds to integer $\hat{p}$ it is an integer in units of p_0.

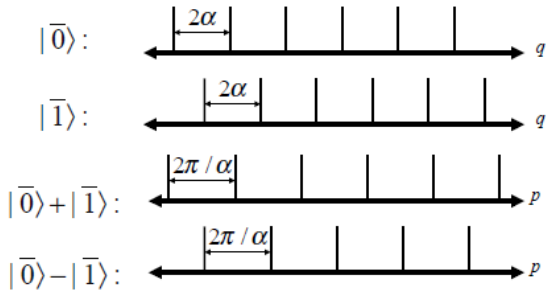

FIG. 3 Picture from (Gottesman *et al.*, 2001): Amplitude of codewords for the stabilizer code with commuting checks $S_q(\alpha) = e^{2i\pi\hat{q}/\alpha}$ and $S_p(\alpha) = e^{-2i\hat{p}\alpha}$ which encodes a qubit in an oscillator.

sufficiently small parameters $\kappa_\pm, \theta, K$ can be expanded into the small shift operators and can thus be corrected. The level of protection thus goes well beyond that of the cat state code.

However, the codewords of this code in Fig. 3 are not physically achievable as it requires an infinite amount of squeezing to prepare (superpositions of) of a quadrature eigenstates such as $|q\rangle$ or $|p\rangle$. (Gottesman *et al.*, 2001) proposed to use approximate codewords: for example the approximate codeword $|\tilde{0}\rangle$ is a superposition of Gaussian peaks in q-space, —each one centered at integer multiples of $2\sqrt{\pi}$ with width Δ—, in a total Gaussian envelope of width $1/\kappa$. Viewed as a superposition of p-eigenstates, such state is a superposition of peaks with width κ and total envelope of width Δ^{-1}. An error analyis of this approximate encoding was done in (Glancy and Knill, 2006), while (Vasconcelos *et al.*, 2010) considered the preparation of the encoded states using cat states as in Eq. (6), squeezing and homodyne detection. In (Menicucci, 2013) the author shows how one can use a continuous-variable cluster state and homodyne measurements to perform quantum error correction on the GKP codewords and realize a universal set of gates assuming that the noise is only due to the finite amount of squeezing in the preparation of the GKP codewords and the cluster state. For squeezing levels of 21dB, the author estimates that the (worst-case) effective gate error-rate is 10^{-6}, sufficiently below the noise threshold of the surface code discussed in Section III.A. In Section III.A.3 we will consider a version of the surface or toric code which encodes an oscillator in a 2D coupled array of harmonic oscillators which can also be viewed as a way to concatenate the GKP code with the surface code.

C. D-dimensional (Stabilizer) Codes

Of particular practical interest are D-dimensional stabilizer codes. These are stabilizer code families on qubits located at vertices of some D-dimensional cubic lattice (with or without periodic boundary conditions). The parity checks involve $O(1)$ qubits which are within $O(1)$ distance of each other on this lattice where $O(1)$ means that this quantity is a constant independent of blocksize n. One can easily prove that one-dimensional stabilizer codes have distance $O(1)$, independent of blocksize (Bravyi and Terhal, 2009), showing that without concatenation, such codes offer little fault-tolerant protection. Various two-dimensional topological stabilizer codes will be discussed in Section III, while some 3D examples of topological codes are the Haah code (Bravyi and Haah, 2013), the Chamon code (Bravyi *et al.*, 2011), the 3D toric code (Castelnovo and Chamon, 2008) and the 4D toric code (Dennis *et al.*, 2002).

There are of course many codes which are not captured by the stabilizer formalism. Here I would like to briefly mention the class of 2D topological qubit codes where the stabilizer checks are still commuting, but they are no longer simple Pauli operators. As Hamiltonians these correspond to the so-called 2D Levin-Wen models (Levin and Wen, 2005), as codes they are called Turaev-Viro codes (Koenig *et al.*, 2010). The advantage of these codes which generalize the 2D surface code in Section III, is that universal quantum computation can achieved by purely topological means. The disadvantage from the coding perspective is that (1) the stabilizer checks are more complicated as operators, e.g. for the so-called Fibonacci code on a hexagonal lattice, the stabilizer checks act on 3 and 12 qubits and (2) decoding and determining a noise-threshold for these codes has only recently begun (Duclos-Cianci and Poulin, 2013; Wootton *et al.*, 2013).

D. Error Correction and Fault Tolerance

We have understood from the previous sections that the crucial element of quantum error correction for stabilizer codes is the realization of the (parity) check measurement as in Fig. 1. The immediate problem is that the parity check measurement suffers from the same imperfections and noise as any other gate or measurement that one may wish to do. In practice a parity check measurement may arise as a continuous weak measurement leaving a classical stochastic data record which hovers around the value $+1$ (pointing to the state being in the code space) while occasionally *jumping* to a value centered around -1, modeled using stochastic master equations (Wiseman and Milburn, 2010). One can imagine that such continuously acquired record is immediately fed back to unitarily steer the qubits to the code space (Ahn *et al.*, 2002). The feedback cannot just rely on the instan-

taneously measured noisy signal or current but should integrate over a longer measurement record to estimate the current conditional quantum state of the system (Wiseman and Milburn, 2010). However, tracking the entire quantum state in real-time is computationally expensive and defeats the purpose of quantum computation. For the realization of quantum error correction, (van Handel and Mabuchi, 2005) describes a filter in which one only tracks the probability that the quantum system at time t is in a state with particular error syndrome $\mathbf{s}$ given the continuous measurement record in time. (Chase *et al.*, 2008) improves on this construction by explicitly including the effect of the feedback Hamiltonian in the stochastic analysis.

Another model of feedback is one in which no (weak) measurements are performed and processed, but rather the whole control loop is a (dissipative) quantum computation. One could set up a simple local error correction mechanism by explicitly engineering a dissipative dynamics which drives/corrects the qubits towards the code space as proposed in (Barreiro *et al.*, 2011; Müller *et al.*, 2011). We assume that the open-system dynamics of code qubits and environment is described by a Lindblad equation as in Eq. (4). For simplicity let us consider the case in which we would like to *pump* or drive four qubits into a state with even parity so that the 4-qubit parity Z-check, $Z_1Z_2Z_3Z_4$ has eigenvalue $+1$. Imagine that we can engineer the dissipation (in the interaction picture) such that there is a single quantum jump operator $L = \sqrt{\kappa}X_1P_{odd}$ with $P_{odd} = \frac{1}{2}(I - Z_1Z_2Z_3Z_4)$, the projector onto the odd parity space, and $H \propto Z_1Z_2Z_3Z_4$. Integration of the Lindblad equation gives rise to the time-dynamics $\rho(t) = \exp(t\mathcal{L}_{tot})(\rho(t=0))$ with stationary states ρ determined by $\mathcal{L}_{tot}(\rho) = 0$. States supported on the even-parity subspace are dark states with $\mathcal{L}(\rho) = 0$ and $[H, \rho] = 0$. The odd-parity subspace is not stationary as the quantum jump operator L flips the first qubit so that an odd parity state becomes an even parity state pumping the system towards the stationary dark subspace.

In (Müller *et al.*, 2011) one considers the following stroboscopic evolution using an ancillary dissipative qubit or mode which approximately gives rise to such Lindblad equation. The idea is to alternate (or *trotterize*) the coherent evolution with H and the dissipative evolution with $\mathcal{L}$ for short periods of time τ so that $\exp(\tau\mathcal{L}_{tot}) \approx \exp(-i\tau[H, .])\exp(\tau\mathcal{L})$. The dynamics of H can be obtained by a small modification of the parity check measurement circuits in Fig. 1 for the evolution $\exp(-i\theta P)$ where P is a multi-qubit Pauli operator we can use the circuit in Fig. 1(b).

The dissipative evolution $\mathcal{L}$ could be implemented for short times $\tau \ll 1$ using a circuit consisting of a dissipative ancilla coupled to the four qubits as in Fig. 1(d). Instead of immediately measuring the ancilla qubit, we apply a CNOT with the ancilla qubit as control and qubit 1 as target (to change the parity of the odd states to even), followed by decay (σ_-) of the ancilla qubit from $|1\rangle$ to $|0\rangle$. These ideas of stabilizer pumping were experimentally tested on two and four ion-trap qubits in (Barreiro *et al.*, 2011). An important disadvantage of this kind of feedback, which we will discuss in Section III.D, is that the correction mechanism is purely *local* in time and space.

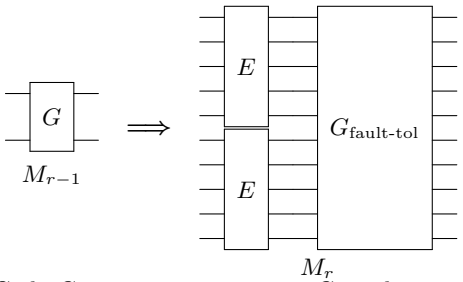

FIG. 4 Code Concatenation: a gate G in the circuit M_{r-1} is replaced by a rectangle consisting of error-correcting steps (E) followed by a fault-tolerant encoded realization of the gate $G_{\text{fault}-\text{tol}}$. The process can be repeated for every elementary gate in the new circuit M_r.

As any realization, closed or open-loop, of quantum error correction will suffer from inaccuracies there is no guarantee that one will improve coherence times by encoding a qubit in a code as it may introduce more errors that it takes away. This has been the reason for the construction of a mathematical theory of quantum fault tolerance which addresses this problem using recursively applied code concatenation. For simplicity, we assume that every such elementary gate, idling step or measurement, —these are called *locations* in the circuit—, can fail independently with some error probability p (independent stochastic noise). In a concatenation scheme every qubit and operation in a quantum circuit is replaced by an encoded qubit and an encoded operation resp. and the process is recursively repeated. The encoded operation consists of an error correction step and a fault-tolerant realization of the operation, see Fig. 4, which together constitute a *rectangle*. For a code such as Steane's $[[7, 1, 3]]$ code which can correct a single error, the fault-tolerance of the rectangle should be such that a single error in any of the locations of the rectangle cannot lead to two (incorrectable) errors in one code block. Then, if the elementary error rate scales as p, it follows that the encoded error rate scales as Cp^2 as two elementary errors are required for a logical error. Here C is a constant which roughly counts the number of pairs of locations in the rectangle where failure can lead to a logical error. If $Cp^2 < p$ the concatenation step helps and r steps of concatenation will drive down the error rate to $\sim p^{2^r}$ while the overhead in terms of qubits and gates increase only exponentially in r. The equality $Cp^2 = p$ sets the *noise threshold* p_c.

This idea of repeated code concatenation was used in

the early days of quantum error correction to prove the *Threshold Theorem* (Aharonov and Ben-Or, 1997; Aliferis *et al.*, 2006; Kitaev, 1997; Knill *et al.*, 1997) which says that fault-tolerant computation is possible with arbitrary small error rate if one is willing to tolerate an overhead which scales polylogarithmically with the *size* N of the computation to be performed (the size of a quantum circuit is the number of locations in it), that is

Theorem 1 *An ideal circuit of size N can be simulated with arbitrary small error δ by a noisy quantum circuit subjected to independent stochastic noise of strength less than $p < p_c$ where the noisy quantum circuit is of size $O(N(\log N)^c)$ with some constant c.*

The important question is of course what is the noise threshold p_c and how large is the constant c? The best performing concatenated coding scheme to date is the C_4/C_6 scheme of Knill (Knill, 2005) for which he estimated a noise threshold as high as $p_c \approx 3\%$ but at the cost of huge overheads. In general, the overhead that one incurs by code concatenation tends to be worse than the overhead (or mere complexity) that is incurred using the idea of topological error correction (Section III), see e.g. the comparative study in (Suchara *et al.*, 2013). One reason is that in topological quantum error correction parity check measurements are simply made robust by repeating the measurement needing no additional qubits. The constant c in the Theorem equals $c = \log_2 S$ where S is the number of locations in a rectangle. For example, in a 2D realization of the concatenated Steane $[[7, 1, 3]]$ code, the fault-tolerant CNOT has $S = O(10^3)$ (Svore *et al.*, 2007) so that $c \approx 10$ demonstrating the potential inefficiency of code concatenation.

One can ask whether it is, in principle, possible to realize fault-tolerant computation with *constant overhead*, meaning that the number of qubits of the noisy fault-tolerant circuit scales with the number of qubits of the original ciruit. This question was analyzed and answered in the affirmative in (Gottesman, 2013). The fault-tolerant construction in (Gottesman, 2013) can be based upon any family of quantum LDPC (low-density parity-check) codes with constant *rate* $R = \frac{k}{n} \geq c$ and, loosely speaking, finite noise-threshold (when the blocksize $n \to \infty$) even if parity check measurements are faulty. LDPC stabilizer qubit codes are codes such that all parity checks (stabilizer generators) acts on O(1) qubits (independent of the blocksize). Several codes with such properties have recently been developed (Freedman and Hastings, 2013; Guth and Lubotzky, 2013; Tillich and Zémor, 2009) which have distances $d = O(n^\alpha)$ with $0 < \alpha \leq 0.5$ which can then be used, see (Gottesman, 2013; Kovalev and Pryadko, 2013) to ensure the code has a finite noise-threshold.

It was proven in (Bravyi *et al.*, 2010) that 2D stabilizer codes (which are LDPC codes with qubits on a 2D regular lattice) obey the tradeoff $kd^2 = O(n)$ demonstrating that 2D codes such as the surface codes discussed in Section III do not allow for fault-tolerant computation with constant overhead. More generally, the results in (Bravyi *et al.*, 2010) show that any D-dimensional stabilizer code family which has distance scaling with lattice size will have a vanishing rate (when $n \to \infty$), showing that non-local parity checks (between $O(1)$ but distant qubits) on such lattices are necessary in order to achieve a constant overhead. We note that it is an open question whether there exist quantum LDPC codes with constant rate and distance scaling as $n^{1/2+\beta}$ for some $\beta > 0$.

E. Universal Quantum Computation

An important feature of error correction with stabilizer (subsystem) codes is the fact that one never physically has to do the correcting Pauli operation *as long as the qubits only undergo Clifford group operations.* The decoding procedure gives a Pauli error which is interpreted as a frame, the so-called Pauli frame (Knill, 2005) which we can efficiently track during the computation using the Knill-Gottesman theorem (Gottesman, 1999b). The Clifford group $\mathcal{C}_n$ is a finite subgroup of the group of unitary transformations $\mathcal{U}(2^n)$ on n qubits. It is defined as the normalizer of the Pauli group: $\mathcal{C}_n = \{U \in \mathcal{U}(2^n) | \forall P \in \mathcal{P}_n, \exists P',\ UPU^\dagger = P'\}$. The generators of the Clifford group are the 2-qubit CNOT gate, the Hadamard H gate, the phase gate S [7] and the Pauli X, Z. The Knill-Gottesman theorem (Gottesman, 1999b) proves that one can efficiently classically simulate any quantum circuit with Clifford group gates. One does this by tracking the stabilizer group, more precisely its generators, which has the input state of the quantum circuit as its unique $+1$ state. Every Clifford gate and measurement maps the stabilizer generators onto new stabilizer generators providing an efficient representation of the action of the quantum circuit. The presence of additional Pauli errors can thus be represented as additional updates of the stabilizer generators.

For universal quantum computation one needs additional gates such as the T gate ($\pi/8$ rotation)[7]. Examples of universal gate sets are $\{H, T, \text{CNOT}\}$, $\{H, \text{Toffoli}\}$ and $\{H, \Lambda(S)\}$ where $\Lambda(S)$ is the two-qubit controlled-S gate [8]. Even though Clifford group gates have no quantum computational power they can be used to develop a *quantum substrate* on which to build universal computation using stabilizer codes. This comes about by combining the following sets of ideas. First of all, note that stabilizer error correction by itself only uses CNOT gates,

---

[7] $H = \frac{1}{\sqrt{2}} \begin{pmatrix} 1 & 1 \\ 1 & -1 \end{pmatrix}$, $S = \begin{pmatrix} 1 & 0 \\ 0 & i \end{pmatrix}$, $T = \begin{pmatrix} 1 & 0 \\ 0 & e^{i\pi/4} \end{pmatrix}$.

[8] $\Lambda(S)|b_1, b_2\rangle = |b_1\rangle S^{b_1} |b_2\rangle$ for $b_1, b_2 = 0, 1$.

preparations of $|+\rangle, |-\rangle, |0\rangle, |1\rangle$ and measurements in the Z- and X-basis as is clear from Fig. 1. The T, $\Lambda(S)$ and the Toffoli gate, each of which can be used with Clifford gates to get universality, are special unitary gates as they map Pauli errors onto elements of the Clifford group. One can define a Clifford hierarchy (Gottesman and Chuang, 1999) $\mathcal{C}(j) = \{U \in \mathcal{U}(2^n) | U\mathcal{P}_n U^\dagger \subseteq C(j-1)\}$ such that $\mathcal{C}(0) = \mathcal{C}(1) = \mathcal{P}_n$, $\mathcal{C}(2) = \mathcal{C}_n$. The $T, \Lambda(S)$ and Toffoli are thus members of $\mathcal{C}(3)$. Such gates in $\mathcal{C}(3)$ (and similarly gates in $C(j)$ for $j > 3$) can be realized with ancillas and Clifford group gates using quantum teleportation ideas (Gottesman and Chuang, 1999; Zhou *et al.*, 2000). The idea is illustrated in Fig. 6 for the T gate. One teleports the qubit on which the T gate has to act, prior to applying the gate, using the bottom one-bit teleportation circuit in Fig. 5. We insert $TT^\dagger$ prior to the corrective Pauli X and note that the T gate can be commuted through the control-line of the CNOT as both gates are diagonal in the Z-basis on the control qubit. Using that $TXT^\dagger = e^{-i\pi/4}SX$ which is an element of the Clifford group, we obtain the circuit in Fig. 6.

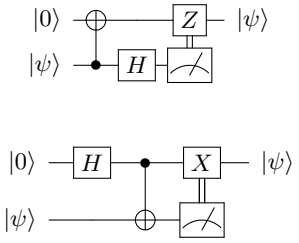

FIG. 5 The so-called one-bit teleportation circuits (Zhou *et al.*, 2000). The measurement denoted by the meter is a measurement in the Z-basis and determines whether to do a Pauli on the output qubit.

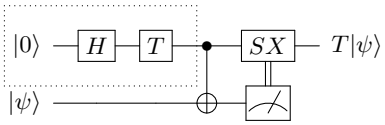

FIG. 6 Using the ancilla $T|+\rangle$ in the dashed box, one can realize the T gate by doing a corrective operation SX.

We can do the same trick for the S gate, that is, we can reduce the S gate to the preparation of a $|+i\rangle = \frac{1}{\sqrt{2}}(|0\rangle + i|1\rangle)$ ancilla, a CNOT gate and a corrective Pauli Y. We get this from starting with the bottom circuit in Fig. 5 to which we apply the S gate at the output. We insert $SS^\dagger$ before the corrective Pauli X and use that $SXS^\dagger \propto Y$. We thus need the ancilla $SH|0\rangle = \frac{1}{\sqrt{2}}(|0\rangle + i|1\rangle)$.

How do we realize a universal set of logical fault-tolerant gates for a code? In principle, fault-tolerant gate constructions can be made for any stabilizer code (Gottesman, 1997). The question is how to do computation with minimal resource requirements and overheads, that is, as close as possible to the resources needed for a quantum memory alone. Ideally, the computation threshold, i.e. the performance of the code when used for computation is close to the memory noise threshold, the performance of the code as a pure quantum memory. An example of a gate which does not require additional qubits is a *transversal* CNOT between two code blocks (each with n qubits) in which every qubit in the block is paired with a qubit in the other block in a CNOT gate such that the encoded CNOT is realized by doing n two-qubit CNOTS in parallel. Such transversal CNOT represents a valid logical CNOT for stabilizer codes $\mathcal{S} = \langle \mathcal{S}(X), \mathcal{S}(Z) \rangle$, i.e. the parity X-checks are the same as parity Z-checks. Examples are Steane's $[[7, 1, 3]]$ code or any other CSS code constructed from a classical code C with $C^\perp \subseteq C$.

In (Bravyi and Koenig, 2013) it was shown for any 2D stabilizer code that the logical gates which can be performed by constant-depth circuits employing only local gates, are members of the Clifford group. The reason to focus on constant-depth local circuits is that such circuits are small and are naturally fault-tolerant. Namely, any number of errors which occurs in the circuit will only affect a patch of $O(1)$ qubits on the 2D lattice, and such $O(1)$ error patches are correctable. Hence we expect that their implementation does not negatively impact the noise threshold or the overhead.

As we will discuss in Section III, one can implement the logical H and CNOT by topological means in the 2D surface code, but one cannot do the logical S gate in this manner. For the surface code one can do the logical S in the same fashion as the logical T, see below (for a different logical S trick, see (Aliferis, 2007)). Other stabilizer codes, 2D color codes, have been found which allow for a topological realization of the full Clifford group (Bombin and Martin-Delgado, 2006). Interestingly, (Bravyi and Koenig, 2013) shows that for D-dimensional stabilizer codes all logical encoded gates which are *composed* from constant-depth logical gates are contained in the Clifford hierarchy $\mathcal{C}(D)$. This is a subtle result as we can realize a fault-tolerant set of universal gates for any stabilizer code, but apparently we cannot do this by composing a sequence of constant-depth encoded gates.

For gates such as the T gate the method of magic-state-distillation has been developed (Bravyi and Kitaev, 2005). This method shows how to realize these gates fault-tolerantly assuming the availability of noiseless Clifford group operations. Thus, once we have built a low-noise Clifford computation substrate, universal quantum computation can be bootstrapped from it. The strength of the distillation scheme is that the noise threshold for it to work is high, approximately 15%. The downside is that the qubit/gate overhead per logical T gate is orders of magnitude larger that of a 'topological' CNOT (see e.g. Fig. 11 in (Raussendorf *et al.*, 2007)). In a nutshell,

the ideas are as follows. We implement the T gate at the logical level using Fig. 6 which requires the preparation of low-noise logical ancillas $\overline{T}|\overline{+}\rangle$. We can obtain such an ancilla in non-fault-tolerant noisy manner by, for example, *injecting* several noisy unencoded ancillas into the code (Knill, 2005). From many of these noisy encoded ancillas we distill using logical H, CNOTs and measurements, a single low-error encoded ancilla.

Note that prior to the action of logical non-Clifford gates one *does* need to physically implement the inferred *logical* Pauli errors obtained from decoding as gates such as the T gate does not map Pauli errors onto Pauli errors but onto Clifford errors. What one never needs to physically do is a correction which maps one back to the $+1$ eigenspace of the stabilizer $\mathcal{S}$: any syndrome eigenspace of $\mathcal{S}$ is a good code. This observation means that for quantum computation with stabilizer codes the rate at which syndromes are processed and errors are inferred should *at least* be the rate at which errors occur. If not, one would acquire an increasing backlog of error syndromes. Such long backlog of error syndromes is problematic as one occasionally has to perform a non-Clifford gate in the quantum circuit and prior to this gate one needs to have physically implemented any *logical* Pauli correction. If there is a substantial syndrome backlog, then one has not yet determined this correct logical Pauli frame. Note that some constant backlog in processing error syndromes can be tolerated as long as the likelihood for a logical error to occur during this time is small. This requirement on the processing of errors may be highly nontrivial to achieve as it means that the time to obtain *and* process a reliable parity check measurement record to infer an error should be much less than the decoherence time of each individual qubit!

The upshot of these considerations is that 2D and 3D stabilizer codes will be most suitable for building a quantum memory and performing Clifford group operations. The goal of universal quantum computation within the same platform can be reached using methods such as injection-and-distillation but the additional overhead and complexity of distillation (and demands for fast decoding) are considerable. Several recent papers have been devoted to reducing this overhead, see e.g. (Jones, 2013a), (Jones, 2013b) and references therein.

III. 2D (TOPOLOGICAL) ERROR CORRECTION

In this section we discuss three stabilizer/subsystem codes in which the parity checks act locally on qubits laid out on a 2D lattice. Two of these codes are topological codes: if the code is defined on a 2D lattice with periodic boundary conditions,—a torus—, then the logical operators would relate to the non-trivial loops around the torus.

In numerical or analytical studies of code performance, one uses simple error models such the independent *depolarizing noise model* to assess the performance of the code. Independent depolarizing noise assumes that every qubit *independently* undergoes a X, Y or Z error with equal probabilities $p/3$ and no error with probability $1-p$. Similarly, if qubits undergo single-, two-qubit gates or measurement and preparation steps, one assumes that the procedure succeeds with probabilty $1-p$ while with total probability p (tensor products of) Pauli X, Y, Z are applied. A related noise model is that of independent X and Z errors in which a qubit can undergo independently an X error with probability p and a Z error with probability p in each timestep. In all three codes the parity checks are either X or Z-like, detecting either Z or X errors. In addition, the parity Z- and X-checks have the same form, so error correction proceeds identically (but simultaneously) for both types of errors.

We will consider codes which encode a single qubit in a block of n qubits with $n = O(L^2)$ with L the linear size of the 2D array. Important parameters of the code performance are the pseudo-threshold $p_c(L)$ which is the error probability at which the elementary error rate p equals the logical error rate for a given size L, the asymptotic threshold $p_c = \lim_{L\to\infty} p_c(L)$ and the logical, X, Z or total, error rate $\overline{p}(p, L)$ which is a function of the block size and the elementary error rate p. For the Bacon-Shor code in Section III.B, the asymptotic threshold $p_c = 0$, hence it is of interest to consider what is the optimal block size for this code. Another interesting class of 2D topological stabilizer codes are the color codes (Bombin and Martin-Delgado, 2006). The color codes offer little practical advantage over the surface code if the goal is to build a quantum memory as some of the parity checks involve more than 4 qubits and the noise thresholds are similar to the surface code, see e. g. (Landahl *et al.*, 2011).

A. Surface Code

The surface code is a version of Kitaev's toric code (Kitaev, 2003) in which the periodic boundaries of the torus have been replaced by open boundaries (Bravyi and Kitaev, 1998; Freedman and Meyer, 2001). Many of its properties and ideas for its use as a quantum memory were first analyzed in the seminal paper (Dennis *et al.*, 2002). The topological 2D realization of the CNOT gate was first proposed in (Bombin and Martin-Delgado, 2009; Raussendorf and Harrington, 2007).

A simple continuous sheet, depicted in Fig. 7, can encode one logical qubit. The linearly-independent parity checks are weight-4 plaquette Z-checks B_p and star X-checks A_s which mutually commute and are modified at the boundary to act on 3 qubits, see Fig. 7. Note that the star operators are just plaquette operators on the dual lattice when interchanging $X \leftrightarrow Z$. The smallest surface code encoding 1 logical qubit which can cor-

rect 1 error is the code $[[13, 1, 3]]$ [9]. $\overline{Z}$ is any Z-string which connects the north and south *rough* boundaries; we can deform this string by multiplication by the trivially-acting plaquette operators. $\overline{X}$ is any X-string (on the dual lattice) connecting the *smooth* east and west boundary. As these strings have to connect boundaries in order to commute with the check operators, their minimum weight is L. Thus for general L, the code parameters are $[[L^2 + (L-1)^2, 1, L]]$.

Using 13 qubits to correct 1 error does not seem very efficient, but the strength of the surface code is not fully expressed in its distance which only scales as the square root of the number of qubits in the block [10].

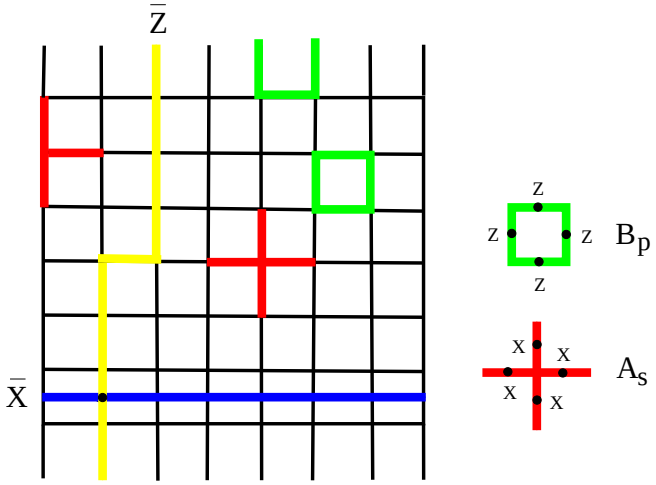

FIG. 7 Surface code on a $L \times L$ lattice. On every edge of the black lattice there is a qubit, in total $L^2 + (L-1)^2$ qubits (depicted is $L = 8$). Two types of local parity checks, A_s and B_p, each act on four qubits, except at the boundary where they act on three qubits. The subspace of states which satisfy the parity checks is two-dimensional and hence represents a qubit. $\overline{Z}$ (yellow) is any Z-string connecting the north to the south boundary, which is referred to as 'rough', while $\overline{X}$ (blue) is any X-string connecting the east to west 'smooth' boundary of the lattice.

Let us consider how quantum error correction can take place first assuming that the parity check measurements are noise-free. If a single X error occurs on an edge in the bulk of the system, then the two plaquette operators next to it will have eigenvalue -1. The places where these plaquette eigenvalues are -1 are called defects. A string of X errors will thus produce two defects at its boundary. If the X error rate p per qubit is sufficiently small, one obtains a low *density* of close-by defects. Such errors are correctable as defects can be locally paired without much ambiguity. As we know, inferring an error E' which differs from the real error E by only stabilizer operators, –plaquette operators in this case–, is harmless. Here it means that we decode correctly as long as $E'E$ does not represent $\overline{X}$, an X-string which goes from one boundary to the other. From this picture it may be intuively clear that there should be a *finite* asymptotic threshold p_c for noise-free error correction.

For the bulk system the error syndrome thus gives us the location of the defects. A minimum-weight decoding algorithm then corresponds to finding a minimum-weight error string $E(X)$ which has these defects as endpoints. This decoding algorithm can be implemented using Edmond's minimum-weight matching (Blossom) algorithm (Edmonds, 1965). Ideal decoding is not minimum weight decoding, but maximum-likelihood decoding as described in Section II.A.1. One can estimate the maximally-achievable threshold p_c with any decoder by relating the maximum likelihood decoding problem to a phase transition in a 2D random-bond Ising model (Dennis *et al.*, 2002; Wang *et al.*, 2003). Assuming noise-free parity checks and independent X errors with probability p, this critical value is numerically estimated as $p_c \approx 11\%$ (Dennis *et al.*, 2002).

This picture gets modified when the parity checks are inaccurate. A simple way to model noisy parity checks is to assign a probability q for the parity check outcome to be inaccurate while in between the parity checks qubits undergo X and Z errors with probability p as before. In practice, one would expect the parity check measurements to induce some correlated errors between the qubits of which we take the parity. For example, for the parity Z-check one may expect to cause additional qubit dephasing when more information than merely the parity is read out.

As the parity check measurements are no longer reliable, one needs to change their use as an error record. For example, a single isolated defect which appears for a few time-steps and then disappears for a long time is more likely due to a faulty parity measurement outcome than due to a string of X errors (which terminates at the isolated defect) that suddenly pops up and disappears without trace after a few time-steps. The strength of topological codes for sufficiently large L (as compared to using small codes and code concatenation) is that noisy parity checks can be dealt with by repeating their measurement as the additional noise which the parity checks produce on the code qubits is local and, at sufficiently low rate, correctable.

Both minimum weight decoding and maximum likeli-

[9] One can minimize the qubit overhead while keeping the distance equal to 3 by rotating the lattice and chopping off some qubits at the corners to get a total of 9 qubits, see e.g. (Horsman *et al.*, 2012).

[10] One can prove that the distance of any 2D stabilizer code is at most $O(L)$ (Bravyi and Terhal, 2009). However, one can also show (Bravyi *et al.*, 2010) that any block of size $R \times R$ where R is less than some constant times the distance, is correctable, i.e. *all* errors in such $R \times R$ patch can be corrected. These arguments show that there are no other 2D stabilizer codes with better distance scaling and that this scaling allows one to correct failed blocks of size beyond the distance.

hood decoding can be generalized to this setting. We extend the lattice into the third (time) dimension (Dennis *et al.*, 2002), see Fig. 8. Vertical links, corresponding to parity check measurements, fail with probability q while horizontal links fail with probability p. In minimum weight decoding the goal is now to find a minimum weight error E which has vertical defect links, where the parity check is -1, as boundary, see Fig. 8. If the parity check measurements are ongoing, one needs to decide how long a record to keep before starting to infer the possible errors; this length depends on the failure probability q. In the simple case when $q = p$ the record length is taken as L (Wang *et al.*, 2003). An analytical lower bound on the noise threshold for $q < p$ is derived in (Dennis *et al.*, 2002) with the value $p_c \geq 1.1\%$. Numerical studies in (Wang *et al.*, 2003) (using minimum weight-decoding) show a threshold of $p_c \approx 2.9\%$ for $p = q$. If we assume that the parity check measurement errors are due to a depolarizing noise model for all elementary gates, measurement and preparations with depolarizing probability p, (Raussendorf *et al.*, 2007) finds a threshold of 0.75%. Below the noise threshold the logical error rate $\overline{p}(p, L) \sim \exp(-\kappa(p)L)$ where $\kappa(p) \approx 0.8 - 0.9$ at $p = p_c/3$ (Raussendorf *et al.*, 2007; Wang *et al.*, 2003). (Wang *et al.*, 2009) even estimates the depolarizing noise threshold to be in the range of $1.1 - 1.4\%$. All these results have been obtained for toric codes, assuming periodic boundary conditions: one may expect results to be somewhat worse for surface codes (Fowler, 2013). These results indicate that the surface code, even with noisy parity check measurements, has a very high threshold as compared to other coding schemes, see e.g. those studied in (Cross *et al.*, 2009) [11] A practically relevant question is how much overhead L is needed before one is in the scaling regime where the pseudo-threshold is close to the asymptotic threshold $p_c(L) \approx p_c$? The pseudo-threshold for a small code such as $[[13, 1, 3]]$ is very tiny, *certainly* no higher than 0.1%. Using the results in (Fowler, 2013), one can estimate that the $[[25, 1, 4]]$ ($L = 4$) surface code has a pseudo-threshold (defined by $\overline{p} = Ap^{L/2}$ with $A = A_X, A_Z$ given in Table I in (Fowler, 2013)) of approximately 0.2% and $[[61, 1, 6]]$ has a pseudo-threshold of approximately 0.7%. Thus a depolarizing error rate $p = 5 \times 10^{-4}$ [[25,1,4]] gives a logical X or Z error rate $\overline{p}_X \approx \overline{p}_Z \approx Ap^2 \approx 1 \times 10^{-4}$ which is barely lower than the bare depolarizing rate. A small Bacon-Shor code will in fact give a better performance (Cross *et al.*, 2009), see the estimate at the end of Section III.B. Even though small surface codes have worse performance than large codes they could still be used as testbeds for individual components and error scaling behavior (Denhez *et al.*, 2012).

[11] One has to be careful in comparing noise threshold values across publications as slightly different methods, noise model, decoding strategy, code usage can impact the results.

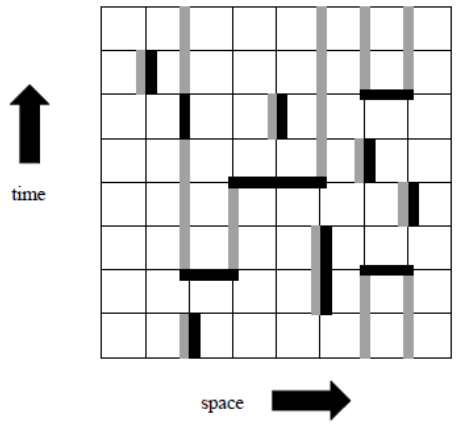

FIG. 8 Picture from (Dennis *et al.*, 2002): 1D cross-section of the lattice in space, and time. Grey links correspond to non-trivial -1 syndromes. Errors which could have caused such a syndrome are represented by black links. Horizontal black links are qubit errors while vertical black links are parity check measurement errors. Note that a possible error E has the same boundary as the grey defect links: a likely error E (in the bulk) can be found by looking for a minimum-weighted matching of the end-points of the grey links.

Minimum-weight decoding with Edmonds' matching algorithm is a good decoding method if our goal is to realize a quantum memory (with or without encoded Clifford group operations). As one never needs to physically do any correction (see the notion of Pauli frame discussed in Section II.E), the measurement record can be stored. This data record can then be processed at leisure and used to interpret a final $M_{\overline{X}}$ or $M_{\overline{Z}}$ measurement on the qubits. The realization of such quantum memory will require that the record of parity check measurements is obtained at sufficiently high rate compared to the error rate, since a low rate stroboscopic picture of the defects (even if they are obtained perfectly) could potentially miss the occurrence of a logical error. Researchers have developed faster renormalization-group decoders (Bravyi and Haah, 2013; Duclos-Cianci and Poulin, 2014) which process the defects using parallel processing over the 2D or 3D lattice in time $O(\log L)$. The idea of the simple decoder in (Bravyi and Haah, 2013) which works for any D-dimensional stabilizer code is to recursively match defects locally. For a 2D surface code with perfect parity check measurements, one starts by dividing up the defect record into local clusters of O(1) size. In each cluster the algorithm tries to find a local error which removes the defect. If a cluster contains a single defect for example, then no such local error can be found. Thus the next step is to enlarge the linear size of the cluster by a factor of 2 and reapply the same procedure on the leftover defect record. The decoder stops when no more defects are present or when one has a reached a certain max-

imum number of iterations $r = O(\log L)$. For the toric code with perfect parity checks, (Bravyi and Haah, 2013) has obtained a noise threshold of $p_c = 6.7\%$ using this RG decoder while the RG decoder in (Duclos-Gianci and Poulin, 2010) achieves 9% (minimum-weight decoding via matching gives 10.3%).

1. Multiple Qubits and Operations by Lattice Surgery

How do we prepare the surface code memory in the states $|\overline{0}\rangle, |\overline{1}\rangle$ or $|\overline{\pm}\rangle$? And how do we read out information, that is, realize $M_{\overline{X}}$ and $M_{\overline{Z}}$? In order to prepare $|\overline{0}\rangle$, we initialize all elementary qubits in Fig. 7 to $|0\rangle$ and start measuring the parity checks. The state $|00\ldots0\rangle$ has $B_p = +1$ and $\overline{Z} = +1$ while the star operators A_s have random eigenvalues ±1 corresponding to the presence of many Z errors. Thus we choose some correction E for these Z errors (we pick a Pauli frame): the choice will not matter as E commutes with $\overline{Z}$. If the preparation of $|0\rangle$ and the parity check measurements are noisy, one needs to measure the parity checks for a while before deciding on a Pauli frame for both X and Z errors. The preparation of $|\overline{1}\rangle$ and $|\overline{\mp}\rangle$ can be performed analogously using the ability to prepare the elementary qubits in $|1\rangle$ and $|\pm\rangle$ respectively. Instead of preparing the quantum memory in one of these four fixed states, there are also methods for encoding a single unencoded qubit $|\psi\rangle$ into a coded state $|\overline{\psi}\rangle$, see (Dennis *et al.*, 2002; Horsman *et al.*, 2012). Of course, during this encoding procedure, the qubit to be stored is not fully protected, as the qubit starts off in a bare, unencoded state.

A projective (non-QND) measurement in, say, the $|\overline{0}\rangle, |\overline{1}\rangle$-basis ($M_{\overline{Z}}$) proceeds essentially in reverse order. One measures all qubits in the Z-basis. Using the past record of parity Z-check measurements and this last measurement, one infers what X errors have taken place and corrects the outcome of $\overline{Z} = \pm1$ accordingly.

There are various ways in which we can encode multiple qubits in the surface code and do a logical Hadamard and CNOT gate. The simplest and most efficient method in terms of qubit overhead is to encode multiple qubits in multiple separate sheets (as in Fig. 7) laid out next to each other in a 2D array as in Fig. 11. Using operations on a single sheet one can do a logical Hadamard gate (Dennis *et al.*, 2002). A CNOT between qubits in separate sheets can be realized using the idea of lattice surgery in which sheets are merged and split as proposed in (Horsman *et al.*, 2012). The important point of doing a CNOT and Hadamard gate using these code deformation methods is that their implementation does not affect the surface noise threshold as error correction is continuously taking place during the implementation of the gates and the single qubit noise-rate is not substantially changed.

We first consider the Hadamard gate for which $\overline{HXH} = \overline{Z}$ and $\overline{HZH} = \overline{X}$. Consider doing a Hadamard rotation on every elementary qubit on a sheet encoding one logical qubit. The resulting state is a $+1$ eigenstate of the Hadamard-transformed parity checks $HA_sH^\dagger$ and $HB_pH^\dagger$ which are the plaquette Z-check resp. the star X-check of the code $\mathcal{S}_{dual}$ defined on the dual lattice. The Hadamard gates map $\overline{Z}$ onto $\overline{X}_{dual}$ and $\overline{X}$ onto $\overline{Z}_{dual}$. In the dual code $\mathcal{S}_{dual}$ the rough and smooth boundaries are interchanged so that the lattice is effectively rotated by 90°. In order to complete the Hadamard gate and return back to the original code one can modify the parity checks at boundaries such that rough becomes smooth and smooth becomes rough again, see the details in (Dennis *et al.*, 2002; Horsman *et al.*, 2012).

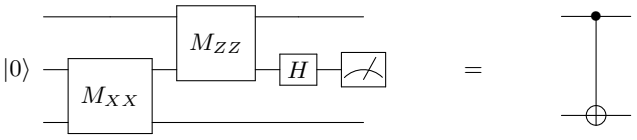

FIG. 9 CNOT via 2-qubit quantum measurements. Here M_{XX} measures the operator $X \otimes X$ etc. The ancilla qubit in the middle is discarded after the measurement in the $\pm$-basis disentangles it from the other two input qubits. Each measurement has equal probability for outcome ±1 and Pauli corrections (not shown, see Eq. (8)) depending on these measurement outcomes are done on the output target qubit.

The construction for the CNOT is based on the circuit in Fig. 9 which implements the CNOT gate through 2-qubit parity measurements, originally described in (Gottesman, 1999a). One could verify Fig. 9 by considering the input states as a stabilizer subspace with stabilizer Z_2 and logical operators $\overline{X}_1, \overline{Z}_1, \overline{X}_3, \overline{Z}_3$, using the Knill-Gottesman simulation technique, see Section 7 in (Gottesman, 1999b). One can also consider the evolution of the input $|c\rangle_1|0\rangle_2|t\rangle_3$ for bits $c = 0, 1$ and $t = 0, 1$ explicitly (here 1 denotes the top qubit in the Figure). For $M_{XX} = +1$, we have a bit $b_{xx} = 0$ and $M_{XX} = -1$ corresponds to $b_{xx} = 1$ etc. We have

$$\begin{aligned} |c\rangle_1|0\rangle_2|t\rangle_3 &\xrightarrow{M_{XX}} Z_3^{b_{xx}} X_3^t |c\rangle_1 \frac{1}{\sqrt{2}}(|00\rangle_{23} + |11\rangle_{23}) \\ &\xrightarrow{M_{ZZ}} Z_3^{b_{xx}} X_3^t |c\rangle_1 X_2^{b_{zz}} |c\rangle_2 X_3^{b_{zz}} |c\rangle_3 \\ &\xrightarrow{M_X} |c\rangle_1 Z_2^{m_x} |+\rangle_2 Z_3^{b_{xx}} X_3^{b_{zz}} |c \oplus t\rangle_3. \quad (8) \end{aligned}$$

We observe the logic of the CNOT gate on qubits 1 and 3 in addition to corrective Pauli's $Z_3^{b_{xx}} X_3^{b_{zz}}$ which depend on the outcomes b_{xx} and b_{zz} of the measurements M_{XX} and M_{ZZ} respectively. The measurement M_X on the second qubit ensures that no information leaks to that qubit so that the CNOT gate properly works on any superposition of inputs.

This circuit identity implies that we can realize a logical CNOT gate if we have the capability of projectively measuring the operators $\overline{X} \otimes \overline{X}$ and $\overline{Z} \otimes \overline{Z}$ of two qubits encoded in different sheets. The capability to prepare a sheet in $|\overline{0}\rangle$ and the measurement $M_{\overline{X}}$ was discussed

before. The realization of such joint measurement, say, $\overline{X}\otimes\overline{X}$ is possible by temporarily merging the two sheets, realizing the measurement and then splitting the sheets as follows. Consider two sheets laid out as in Fig. 10 where a row of ancillary qubits is prepared in $|0\rangle$ between the sheets. We realize a *rough* merge between the sheets by including the parity checks, plaquette and star operators, at this boundary. If the parity check measurements are perfect, the new weight-4 plaquette Z-checks have $+1$ eigenvalue as the ancilla qubits are prepared in $|0\rangle$. The 4 new star boundary checks have random ±1 eigenvalues subject to the constraint that the product of these boundary checks equals the product of $\overline{X}$s of the two sheets. Hence a perfect measurement would let us do a $\overline{X}\otimes\overline{X}$ measurement. As the parity check measurements are imperfect, one needs to repeat the procedure in the usual way to reliably infer the sign of $\overline{X}\otimes\overline{X}$. We are however not yet done as we wish to realize a projective $\overline{X}\otimes\overline{X}$ measurement on the qubits encoded in two *separate* sheets. This means that we should split the two sheets again: we can do this by reversing the merge operation and measure the ancillary qubits in the Z-basis and stop measuring the 4 boundary X-checks. Again, if the parity check measurements are perfect, the eigenvalues of the plaquette Z-checks at the boundary of both sheets will take random values, but both are correlated with the outcome of the Z-measurement on the ancillary qubits. Hence the individual $\overline{X}$ eigenvalues of the separate sheets may be randomized, but they are correlated so that $\overline{X}\otimes\overline{X}$ remains fixed. Similarly, a smooth merging and splitting (as between qubits C and INT in Fig. 11) with the ancillary qubits prepared and measured in the X-basis accomplishes a $\overline{Z}\otimes\overline{Z}$ measurement.

The procedure for a CNOT in Fig. 11 then consists of: first a preparation of the INT qubit in $|\overline{0}\rangle$, then a rough merge and split of qubits T and INT followed by a smooth merge and split between qubits INT and C followed by a final $M_{\overline{X}}$ measurement of qubit INT.

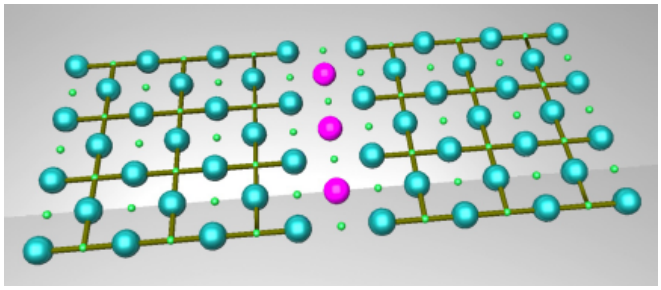

FIG. 10 Picture from (Horsman *et al.*, 2012): two sheets are merged at their rough boundary by placing a row of ancilla qubits in the $|0\rangle$ state at their boundary and measuring the parity checks of the entire sheet. For a similar smooth merge, the ancillary qubits in between the two sheets are prepared in the $|+\rangle$ state, see the INT and C sheets in Fig. 11.

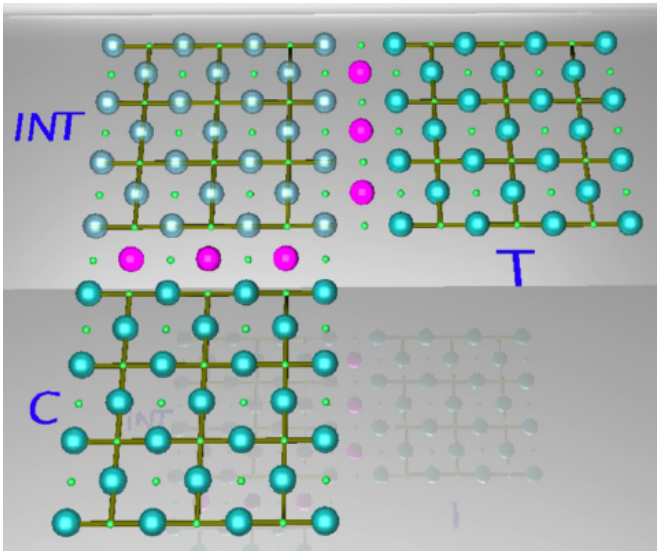

FIG. 11 Picture from (Horsman *et al.*, 2012): using an ancilla (INT) qubit sheet we can do a CNOT between the control (C) and target sheet (T) by a sequence of mergings and splittings between the sheets.

2. Topological Qubits and CNOT via Braiding

A different way of encoding multiple qubits and realizing a CNOT gate was first proposed in (Bombin and Martin-Delgado, 2009; Raussendorf *et al.*, 2007). The disadvantage of this method is that it has an additional qubit overhead. A distance-3 smooth hole qubit (see the description below) costs many more than 13 physical qubits but such overhead could also lead to greater robustness.

In order to see how to encode multiple qubits, we start with a simple square sheet with all smooth boundaries which encodes no qubits, Fig. 12(a) [12]. To encode qubits one makes a *hole* in the lattice, that is, one removes some checks from the stabilizer $\mathcal{S}$. This is a change in topology which affects the code space dimension. In stabilizer terms: when we remove one plaquette, say, B_{p_*} for some p_* from the stabilizer $\mathcal{S}$, then B_{p_*} is no longer an element in $\mathcal{S}$ but still commutes with $\mathcal{S}$, therefore B_{p_*} is a logical operator. The matching logical operator which anti-commutes with it starts at the hole and goes to the boundary. This encoded qubit has poor distance namely $d = 4$ as B_{p*} is of weight 4. We can modify this procedure in two ways such that logical qubits have a large distance and its logical operators do not relate to the boundary. The particular choice of logical qubits will allow one to do a CNOT by moving holes.

[12] On a $L \times L$ lattice there are $2L(L+1)$ qubits, $L^2 + (L+1)^2$ stabilizer checks and one linear dependency between the star operators, hence zero encoded qubits

To get a logical qubit with large distance we simply make a bigger hole. We remove all, say, k^2 plaquette operators in a block (and all $(k-1)^2$ star operators acting in the interior of this block) and modify the star operators at the boundary to be weight-3, no longer acting on the qubits in the interior, see Fig.12(a). The qubits in the interior of the block are now decoupled from the code qubits. The procedure creates one qubit with $\overline{Z}$ equal to any Z-loop around the hole. The $\overline{X}$ operator is a X-string which starts at the boundary and ends at the hole. Clearly, the distance is the minimum of the perimeter of the hole and the distance to the boundary. We call this a *smooth* hole as the hole boundary is smooth. Of course, we could do an identical procedure to the star operators, removing a cluster of stars and smaller subset of plaquette operators and adapting the plaquette operators at the boundary. Such qubit will be called a *rough* hole and its $\overline{X}$ operator is a X-string around the hole (a string on the dual lattice) and $\overline{Z}$ is a Z-string to the boundary.

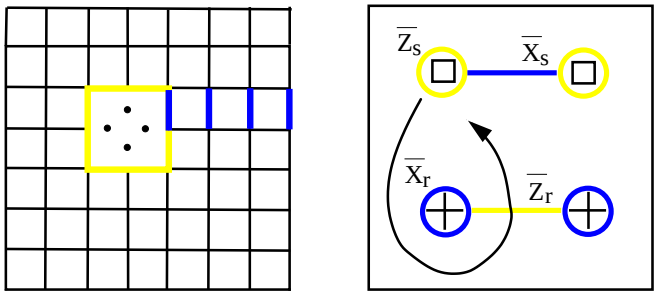

FIG. 12 (a) A smooth hole is created by removing a block of plaquette operators and the star operators acting on qubits in the interior of the block. The Z-loop around the hole is $\overline{Z}$ while $\overline{X}$ is an X-string to the boundary. The qubits inside the hole (4 in the picture) are decoupled from the lattice. (b) Two smooth holes can make one smooth qubit and two rough holes can make one rough qubit so that moving a smooth hole around a rough hole realizes a CNOT gate.

In order to be independent of the boundary, we use two smooth holes to define one *smooth or primal qubit* and use two rough holes to define one *rough or dual qubit* as follows. Consider two smooth holes $1, 2$ and define a new smooth qubit as $|\overline{0}\rangle_s = |\overline{0},\overline{0}\rangle_{1,2}$ and $|\overline{1}\rangle_s = |\overline{1},\overline{1}\rangle_{1,2}$. For this smooth qubit s we have $\overline{Z}_s = \overline{Z}_i, i = 1, 2$ (we can deform $\overline{Z}_1$ into $\overline{Z}_2$ by plaquette operators) and $\overline{X}_s = \overline{X}_1\overline{X}_2$ which we can deform to an X-string which connects the two holes, see Fig. (12)(b). The distance of this smooth qubit is the minimum of the distance between the holes and the perimeter of one of the holes (assuming the boundary is sufficiently far away). Similarly, we can create a *rough* qubit by taking two rough holes and defining

$$|\overline{0}\rangle_r = \frac{1}{\sqrt{2}}\left(|\overline{0},\overline{0}\rangle_{3,4} + |\overline{1},\overline{1}\rangle_{3,4}\right),$$
$$|\overline{1}\rangle_r = \frac{1}{\sqrt{2}}\left(|\overline{0},\overline{1}\rangle_{3,4} + |\overline{1},\overline{0}\rangle_{3,4}\right).$$

With this choice $\overline{X}_r$ is the loop $\overline{X}_3$ (or equivalently $\overline{X}_4$) while $\overline{Z}_r = \overline{Z}_1\overline{Z}_2$ is equivalent to the Z-string connecting the holes.

Imagine moving one smooth hole around a rough hole as in Fig. 12(b). After the move, the X-string connecting the smooth holes will additionally go around the rough hole enacting the transformation $\overline{X}_s \to \overline{X}_r \otimes \overline{X}_s$. This can be understood by noting that an $\overline{X}$-string with some endpoints a and b which loops around a rough hole is equivalent (modulo stabilizer operators) to an $\overline{X}$-loop around the rough hole disconnected from a direct $\overline{X}$-string between the endpoints a and b. Similarly, the Z-string $\overline{Z}_r$ connecting the rough holes wil, after the move, wind around the smooth hole, leading to the transformation $\overline{Z}_r \to \overline{Z}_s \otimes \overline{Z}_r$. The loops $\overline{Z}_s$ and $\overline{X}_r$ are not changed by the move. This action precisely corresponds to the action of a CNOT with smooth qubit as control and rough qubit as target [13].

The ability to do a CNOT with a smooth qubit as control and a rough qubit as target qubit seems limited as all such gates commute. However one can use the one-bit teleportation circuits in Fig. 5 to convert a smooth qubit into a rough qubit and a rough qubit into a smooth qubit, using *only* CNOTs with smooth qubits as controls. We have already shown how to realize the other components in the one-bit teleportation circuit such as $M_{\overline{X}}$ and $M_{\overline{Z}}$. Thus by composing these circuits we can do a CNOT between smooth qubits alone (or rough qubits alone).

How is the braiding done using elementary gate operations? The advantage of realizing topological gates in stabilizer codes (as opposed to braiding of Majorana fermions or non-Abelian anyons in quantum Hall systems) is that braiding can be realized by changing where we measure the parity checks, or *deforming the code*. For example, one can enlarge the hole in Fig. 12 to include, say, 2 more plaquettes and 3 more qubits in the interior. We stop measuring those two plaquette checks and the star checks in the interior, modify the star boundary measurements and measure the qubits in the interior in the X-basis. The modified weight-3 boundary checks will have random ± 1 eigenvalues as their previous eigenstates were perfectly entangled with the qubits in the interior. This corresponds to a high Z-error rate around the modified boundary. By repeating the measurement to increase

[13] The action of the CNOT in the Heisenberg representation is $X_c \otimes I_t \to X_c \otimes X_t$, $I_c \otimes X_t \to I_c \otimes X_t$, $Z_c \otimes I_t \to Z_c \otimes I_t$ and $I_c \otimes Z_t \to Z_c \otimes Z_t$ where X_c (X_t) stands for Pauli X on control qubit c (t) etc.

the confidence in their outcome one can correct these Z-errors, but of course we may partially complete a $\overline{Z}$-loop this way. The protection against a full $\overline{Z}$-loop around the hole is thus provided by *the part of the hole boundary which remains fixed.*

This implies that the hole can safely be moved and braided in the following *caterpillar* manner. One first enlarges the hole (while keeping its 'back-end' fixed providing the protection) so that it reaches its new position. In terms of parity check measurements it means that from one time-step to the next one, one switches from measuring the small hole to the large hole parity checks. Due this extension errors will occur along the path over which the hole is moved and if error correction is noisy we should not act immediately to infer the new Pauli frame, but repeat the new check measurements to make this new frame more robust. Then as a last step, we shrink the hole to its new position and corroborate the new measurement record by repetition. Alternatively, one can move the hole by a sequence of small translations, so that the hole never becomes large. The speed at which the hole can then be safely moved is determined by the time it takes to establish a new Pauli frame (eliminate errors) after a small move. Details of hole moving schemes are discussed in e.g. (Fowler *et al.*, 2009).

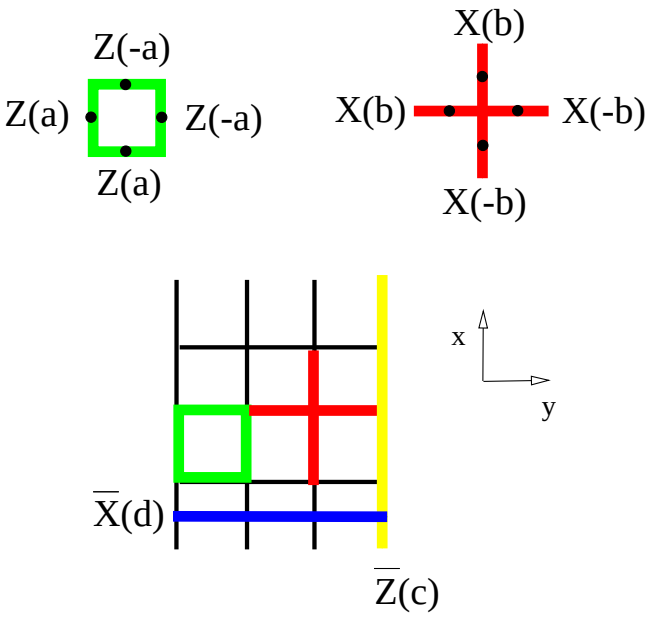

FIG. 13 Small example of the oscillator surface code where oscillators on the edges are locally coupled with plaquette and star operators so as to define an encoded oscillator with logical, non-local, displacements $\overline{X}(d)$ and $\overline{Z}(c)$. The realization of the four-oscillator interaction will require strong 4-mode sqeezing in either position (at plaquettes) or momenta (at stars).

3. Surface Code with Harmonic Oscillators

It is possible to define a qudit stabilizer surface code, see e.g. (Bullock and Brennen, 2007), where the elementary constituents on the edges of the lattice are qudits with internal dimension d and the code encodes one or several qudits. An interesting special case is when we take $d \to \infty$ and each edge is represented by a harmonic oscillator with conjugate variables $\hat{p}, \hat{q}$. The goal of such continuous-variable surface code is to encode a non-local oscillator into an 2D array of oscillators such that the codestates are protected against local shifts in $\hat{p}$ and $\hat{q}$. In addition, one can imagine using continuous-variable graph states to prepare such encoded states and observe anyonic statistics (Zhang *et al.*, 2008).

To get a surface code, we replace Pauli X by $X(b) = \exp(2\pi i b\,\hat{p})$ and Pauli Z by $Z(a) = \exp(2\pi i a\,\hat{q})$ with real parameters such that $Z^\dagger(a) = Z^{-1}(a) = Z(-a)$ etc. It follows that for any two qubits 1 and 2, we have

$$\forall a, b,\ [Z_1(a)Z_2(-a), X_1(b)X_2(b)] = 0. \qquad (9)$$

In the bulk of the surface code lattice, a plaquette operator centered at site p can be chosen as $B_p(a) = Z_{p-\hat{x}}(a)Z_{p+\hat{x}}(-a)Z_{p-\hat{y}}(a)Z_{p+\hat{y}}(-a)$ while a star operator is equal to $A_s(b) = X_{s-\hat{x}}(-b)X_{s+\hat{x}}(b)X_{s-\hat{y}}(b)X_{s+\hat{y}}(-b)$, see Fig. 13.

Here $Z_{p-\hat{x}}(a) = \exp(2\pi i a\,\hat{q}_{p-\hat{x}})$ where $\hat{q}_{p-\hat{x}}$ is the position variable of the oscillator at site $p-\hat{x}$ ($\hat{x}$ and $\hat{y}$ are orthogonal unit-vectors on the lattice). One can observe from the Figure and Eq. (9) that $B_p(a)$ and $B_p^\dagger(a)$ commute with $A_s(b)$ and $A_s^\dagger(b)$ for all a, b in the bulk and at the boundary.

We can define Hermitian operators with real eigenvalues in $[-1, 1]$ as $H_p(a) = \frac{1}{2}(B_p(a) + B_p^\dagger(a)) = \cos(2\pi a(q_{p-\hat{x}} - q_{p+\hat{x}} + q_{p-\hat{y}} - q_{p+\hat{y}}))$ and $H_s(b) = \frac{1}{2}(A_s(b)+A_s^\dagger(b)) = \cos(2\pi b(-p_{s-\hat{x}}+p_{s+\hat{x}}+p_{s-\hat{y}}-p_{s+\hat{y}}))$. We now define the code space as the $+1$ eigenspace of all $H_p(a), H_s(b)$ for all a and b. It follows that a states in the code-space is a delta-function in the positions of the oscillators around all plaquettes p, that is, $\delta(q_{p-\hat{x}} - q_{p+\hat{x}} + q_{p-\hat{y}} - q_{p+\hat{y}})$ for every p, while it is a delta-function in the momenta of the oscillators $\delta(-p_{s-\hat{x}} + p_{s+\hat{x}} + p_{s-\hat{y}} - p_{s+\hat{y}})$ located at all stars s.

One can compare such highly-entangled code state with its simpler cousin, the 2-mode EPR-state. In the 2-mode case we have two commuting operators namely $Z_1(a)Z_2(-a)$ and $X_1(b)X_1(b)$ on oscillator 1 and 2. The single state which is the $+1$ eigenstate of $\cos(2\pi a(q_1 - q_2))$ and $\cos(2\pi b(p_1 + p_2))$ for all a, b is the two-mode infinitely-squeezed EPR state $\delta(p_1 + p_2)\delta(q_1 - q_2)$.

Unlike in the two-mode case, the oscillator surface code space is not one-dimensional, but infinite-dimensional as it encodes a non-local oscillator. The operators $\overline{Z}(c) = \exp(2\pi i c \sum_{i\in\gamma_1} \hat{q}_i)$ where the path γ_1 runs straight from north to south commute with all $H_p(a), H_s(b)$, see Fig. 13. Similarly, we have $\overline{X}(d) = \exp(2\pi i d \sum_{j\in\gamma_2} \hat{p}_j)$

where γ_2 runs straight from east to west. As $\overline{Z}(c)\overline{X}(d) = e^{-i(2\pi c)(2\pi d)}\overline{X}(d)\overline{Z}(c)$, we can interpret $\overline{Z}(c)$ and $\overline{X}(d)$ as phase-space displacements of the encoded oscillator with logical position and momentum $\overline{p} = \sum_{i\in\gamma_2} p_i$ and $\overline{q} = \sum_{i\in\gamma_1} q_i$. We can deform these non-unique logical operators to follow deformed paths, e.g. multiply $\overline{Z}(c)$ by $B_p(c)$ plaquettes (note that if we multiply by $B_p(c')$ with $c' \neq c$ we get an operator with the union of supports).

How would one use such a code to encode quantum information and what protection would it offer? As its qubit incarnation, a sufficiently-low density of independent errors on the lattice can be corrected. For the array of oscillators or bosonic modes, one would instead expect that each oscillator i will independently suffer from small dephasing, photon loss etc., that is, errors which can be expanded into small shifts $Z_i(e)X_i(e')$ with $|e|, |e'| \ll 1$, see Section II.B.1. This means that the likelihood for logical errors of the form $\overline{Z}(c)\overline{X}(d)$ for small c, d will be high which relates of course to the fact that we are attemting to encode a continuous variable rather than a discrete amount of information.

However, one can imagine using only a 2-dimensional subspace, in particular the codewords of the GKP qubit-into-oscillator code, see II.B.1 for each oscillator in the array. One can also view this as a concatenation of the GKP code and the surface code in which we express the surface code plaquette and star operators in terms of the operators on the elementary oscillators in the array. One could prepare the encoded states $|\overline{0}\rangle, |\overline{1}\rangle, |\overline{+}\rangle, |\overline{-}\rangle$ of the surface code by preparing each local oscillator in the qubit-into-oscillator logical states $|0\rangle, |1\rangle, |+\rangle, |-\rangle$ and subsequently projecting onto the perfectly correlated momenta and position subspace. For example, the state $|0\rangle$ of a local oscillator i is an eigenstate of $S_q(\alpha) = e^{2\pi i\hat{q}_i/\alpha}$, $S_p = e^{-2i\hat{p}_i\alpha}$ and the local $\overline{Z}_i = e^{i\pi\hat{q}_i/\alpha}$. This implies that after projecting onto the space with $H_p(a) = 1, H_s(b) = 1$ for all a, b, it will be an eigenstate of $\overline{Z}(1/(2\alpha)) = e^{i\pi\sum_{i\in\gamma_1}\hat{q}_i/\alpha}$, i.e. the encoded $|\overline{0}\rangle$.

B. Bacon-Shor Code

An interesting family of subsystem codes are the Bacon-Shor codes (Bacon, 2006) which are competitive with the surface code for small numbers of qubits. For the $[[n^2, 1, n]]$ Bacon-Shor code the qubits are laid out in a 2D $n \times n$ square array, see Figs. 2 and 14. The stabilizer parity checks are the double Z-column operators $\mathbf{Z}_{||,i}$ for columns $i = 1, \ldots n-1$ and double X-row operators $\mathbf{X}_{=,j}$ for rows $j = 1, \ldots n-1$. It is also possible to work with asymmetric Bacon-Shor codes with qubits in a $n \times m$ array. Asymmetric codes can have better performance when, say, Z errors are more likely than X errors (when $T_2 \ll T_1$), see (Brooks and Preskill, 2013). The gauge group $\mathcal{G}$ (see Section II.A.1) is generated by weight-2 vertical XX links and horizontal ZZ links and contains the parity checks. The logical operators (which commute with $\mathcal{G}$ but are not in $\mathcal{S}$) are the single Z-column $\overline{Z}$ and a single X-row $\overline{X}$.

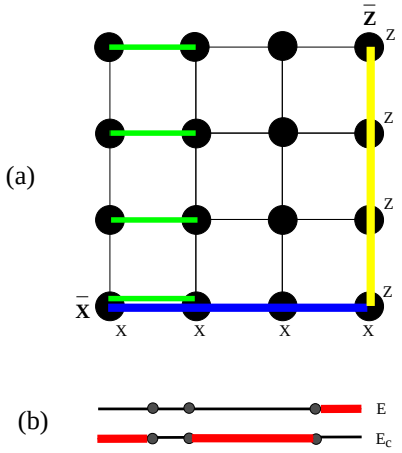

FIG. 14 (a) $[[25, 1, 5]]$ Bacon-Shor code with $\overline{X}$, a row of Xs (blue), and $\overline{Z}$, a column of Zs (yellow). The stabilizer generators are double columns of Zs, $\mathbf{Z}_{||,i}$ (one is depicted) and double rows of Xs, $\mathbf{X}_{=,j}$.(b) Decoding for X errors (or Z errors in the orthogonal direction). Black dots denote the places where the double column parity checks $\mathbf{Z}_{||,i}$ have eigenvalue -1 (defects). The X error string E has X errors in the red region and no errors elsewhere and E_c is its complement. Clearly the string E has lower weight than E_c and is chosen as the likely error.

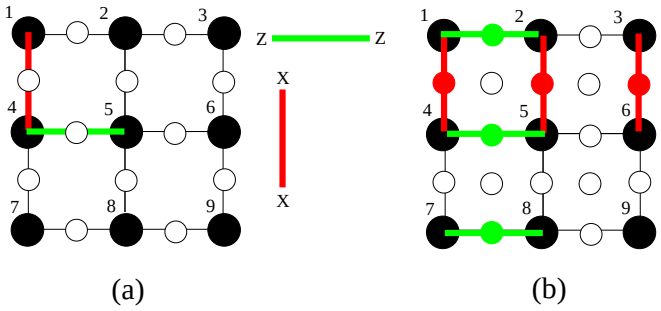

FIG. 15 (a) In order to measure the XX and ZZ operators one can place ancilla qubits (open dots) in between the data qubits. Such ancilla qubit interacts with the two adjacent data qubits to collect the syndrome. (b) Alternatively, to measure $\mathbf{Z}_{||,i}$ one can prepare a 3-qubit entangled cat state $\frac{1}{\sqrt{2}}(|000\rangle + |111\rangle)$ (green dots) which interacts locally with the adjacent system qubits. $\mathbf{X}_{=,1}$ could be measured by preparing a cat state for the ancilla qubits at, say, the red dots. The ancilla qubits at the open dots can be used to prepare the cat states.

Consider the correction of X errors sprinkled on the lattice, assuming for the moment that the parity check measurement of $\mathbf{Z}_{||,i}$ is noise-free. For each column we note that an even number of X errors is a product of the vertical XX gauge operators and therefore does not

affect the state of the logical qubit. This means that per column only the parity of the number of X errors is relevant. The double column operator $\mathbf{Z}_{||,i}$ determines whether this parity flips from column i to column $i+1$. The interpretation of the eigenvalues of $\mathbf{Z}_{||,i}$ is then the same as for a 1D repetition code (or 1D Ising model) with parity checks Z_iZ_{i+1}. Double columns where $\mathbf{Z}_{||,i} \equiv Z_iZ_{i+1} = -1$ are *defects* marking the end-points of X-strings (domain walls in the 1D Ising model). Minimum-weight decoding is very simple as it corresponds to choosing the minimum weight one between two possible X-error strings: E or the complement string E_c which both have the faulty double columns defects as end-points, see Fig. 14(b). The code can thus correct all errors of weight at most $\lfloor \frac{n}{2} \rfloor$ for odd n. Higher-weight errors can also be corrected as long they induce a low density of defects on the boundary. Note however that the number of syndrome bits scales as n whereas the number of errors scales with n^2. This means that in the limit $n \to \infty$ the noise-free pseudo-threshold $p_c(n) \to 0$ as the fraction of incorrectable errors will grow with n. So, how do we choose n in order to minimize the logical error rate $\overline{p}(p,n)$? In (Napp and Preskill, 2013) the authors find that the optimally-sized Bacon-Shor code for equal X and Z error rate p is given by $n = \frac{\ln 2}{4p}$ and for that optimal choice they can bound the logical X (or Z) error rate as $\overline{p}(p) \lesssim \exp(-0.06/p)$.

How does acquire the non-local parity check values? One can either measure the XX and ZZ gauge operators and use this information to get the eigenvalues of $\mathbf{X}_{=,i}$ and $\mathbf{Z}_{||,j}$, or one measures the parity checks directly. The first method has the advantage of being fully local: the ancilla qubits for measuring XX and ZZ can be placed in between the data qubits, see Fig.15(a). In the second method we can prepare an n-qubit cat state, see e.g. (Brooks and Preskill, 2013). We could measure $\mathbf{Z}_{||,1}$ using the circuit in Fig. 1(a) with a single ancilla qubit in the $|+\rangle$ state and controlled-phase gates (CZ) gates. However, a single X error on the ancilla qubit can feed back to the code qubits and cause multiple Z errors making the procedure non fault-tolerant. In addition, the interaction between the ancilla qubit and the code qubits is non-local. Instead, we encode the ancilla qubit $|+\rangle$ using the repetition code, i.e. we prepare the n-qubit cat state $\frac{1}{\sqrt{2}}(|00\ldots0\rangle + |11\ldots1\rangle)$ such that a CZ-gate acts between one cat qubit and one code qubit. The n-qubit cat state, which is stabilized by Z_iZ_{i+1} and $X_1\ldots X_n$, can be made by preparing $|+\rangle^{\otimes n}$ and measuring Z_iZ_{i+1} using local ancilla qubits. The Z_iZ_{i+1} eigenvalues are recorded to provide the Pauli frame. In (Brooks and Preskill, 2013) further details of this scheme are given, including estimates of the noise threshold for asymmetric Bacon-Shor codes.

Consider now the first method of directly measuring XX and ZZ: what happens when the local XX and ZZ checks are measured inaccurately? The good news is this only causes *local* errors on the system qubits. The bad news is that if the measurement outcome of, say, XX has some probability of error q, then the error probability for a nonlocal stabilizer check $\mathbf{X}_{=,i}$. This is a disadvantage of the Bacon-Shor code. Researchers (Aliferis and Cross, 2007; Brooks and Preskill, 2013) have sought to improve the fault-tolerance of the parity check measurements by replacing the preparation of simple single qubit ancillas by fault-tolerant ones (methods by Steane and Knill). In (Aliferis and Cross, 2007) a best noise-threshold of $p_c \approx 0.02\%$ was numerically obtained for the (concatenated) $[[25,1,5]]$ code. (Napp and Preskill, 2013) have considered an alternative way of making the syndrome more robust, namely by simple repetition of the XX and ZZ measurements and a collective processing of the information (as is done for the surface code). We can view the effect of repetition as extending the 1D line of defects to a 2D lattice of defects, as in Fig. 8, so that minimum weight decoding corresponds to finding a minimum weight matching of defect end-points. The error rate for vertical (black) links representing the parity check errors scales with n while the error rate for horizontal links (when one column has an even and the other column has an odd number of errors) scales, for low p, also with n. In (Napp and Preskill, 2013) the authors estimate that the optimal size for the Bacon-Shor code is then $n \approx 0.014/p$ and that for this choice, the logical error rate $\overline{p}(p) \lesssim \exp(-0.0068/p)$. Hence for an error rate of $p = 5 \times 10^{-4}$, we can choose $n = 28$ giving a logical X (or Z) error rate of $\overline{p} \approx 1.25 \times 10^{-6}$.

C. Subsystem Surface Code

The Bacon-Shor code shows that it is possible to reduce the requirement to measure 4-qubit parities by using subsystem codes. One can prove that 2D qubit codes defined as eigenspaces of at most 3-local (involving at most 3 qubits) mutually commuting terms are trivial as quantum codes (Aharonov and Eldar, 2011), hence it is also necessary to use subsystem codes if the goal is to have lower-weight, and hence less noisy, parity checks with 2D codes. The Bacon-Shor code is however not a topological subsystem code as the stabilizer checks are nonlocal on the 2D lattice and its asymptotic noise threshold is vanishing.

Several topological subsystem codes have been proposed in which weight-2 parity checks are measured (Bombin, 2010), but the asymptotic noise threshold for such codes is typically quite a bit lower than for the surface code, see e.g. (Suchara *et al.*, 2011).

In (Bravyi *et al.*, 2013) a topological subsystem code was proposed,—a subsystem surface code—, in which the non-commuting parity checks are of weight-3 and the stabilizer generators are of weight 6, see Fig. 16.

More precisely, the gauge group $\mathcal{G}$ is generated by the triangle operators XXX and ZZZ, including cut-off weight-2 operators at the boundary. The stabilizer group $\mathcal{S} = \mathcal{G} \cap \mathcal{C}(\mathcal{G})$ is generated by weight-6 plaquette operators (at the boundary $\rightarrow$ weight-2 operators). By measuring, say, the Z-triangles we can deduce the eigenvalues of the Z-plaquettes which are used to do error correction.

For a $L \times L$ lattice one has a total of $3L^2 + 4L + 1$ qubits and $2L^2 + 4L$ independent stabilizer generators which gives $L^2 + 1$ qubits. One of these qubits is the logical qubit whose $\overline{Z}$ and $\overline{X}$ commute with all Z and X-triangles. Similar as in the surface code, a vertical Z-line through $2L$ qubits can realize $\overline{Z}$ while a horizontal X-line realizes $\overline{X}$. The logical operators for the L^2 gauge qubits, one for each plaquette, are pairs of triangle operators on a plaquette generating the group $\mathcal{G}$. One can multiply, say, the vertical Z-line by Z-triangles to become a $\overline{Z}$ which acts only on L qubits: in (Bravyi *et al.*, 2013) it is indeed proved that the distance of the code is L. Note that such weight-L $\overline{Z}$ acts on the logical qubit *and* the irrelevant gauge qubits.

For a code with distance $L = 3$ one thus needs 41 elementary qubits, substantially more than for the surface code. Multiple qubits can be encoded in this subsystem code by making holes as for the surface code. One can expect that braiding and lattice surgery methods for this code can be established in the same way as for the surface code. The interesting feature of this code are its relatively-high noise threshold obtained by reduced-weight parity checks (at the price of a bit more overhead). Decoding of stabilizer syndrome information is done by interpreting the syndrome as defects on a virtual lattice which can processed, similar as for the surface code, by minimum weight matching of defects or by RG decoding. For noise-free perfect error correction and independent X, Z noise, the authors report a maximum threshold of $p_c \approx 7\%$ (compare with 11% for the surface code). For noisy error correction the threshold depends on how single errors with probability p in the parity check circuit affect the error rate on the virtual lattice. Modeling this effective noise-rate on the virtual lattice, the authors find a noise threshold of $p_c \approx 0.6\%$.

It is not surprising that decoding for the subsystem surface codes can be done using the decoding method for the surface code. It was proved in (Bombin *et al.*, 2012) that any 2D topological subsystem or stabilizer code can be locally mapped onto copies of the toric code. The upshot is that for any such code one can find, after removing some errors by local correction, a virtual lattice with toric code parity checks and an underlying effective error model. An example of another 2D topological subsystem code which may be analyzed this way is a concatenation of the $[[4, 2, 2]]$ code with the surface code. If we use the $[[4, 2, 2]]$ code as subsystem code then the concatenated code has weight-2 and weight-8 check operators. The scheme may be of interest if the weight-2 checks can be measured fast and with high accuracy.

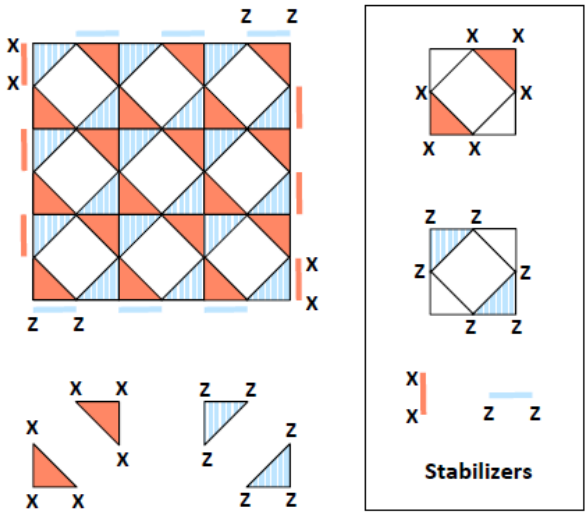

FIG. 16 Picture from (Bravyi *et al.*, 2013): subsystem surface code on a lattice of size $L \times L$ with L^2 square plaquettes (depicted is $L = 3$). The qubits live on the edges and vertices of the plaquettes and are acted upon by weight-3 X and Z-triangle operators (which are modified to become weight-2 operators at the boundary). The stabilizer checks are weight 6 except at the boundary.

D. Decoding and (Direct) Parity Check Measurements

One can ask whether quantum error correction for the surface or other topological codes in $D = 2$ or higher is possible by purely local means. More precisely, is there a non-zero noise threshold p_c when error correction has to be performed by a 2D noisy automaton which 'sits on top' and locally interacts with the surface code qubits (Dennis *et al.*, 2002): the local computing cells in such an automaton would be allowed to communicate between neighboring cells, but the time duration and hence delay due this communication are to be taken into account. The dissipative correction procedure of stabilizer pumping described in Section II.D is an example of a purely local error correction mechanism which does not use any communication.

We can consider what such a mechanism does if we apply it to the toric code discussed in III.A. Imagine a single X error occurs. For the toric code, such an X error is heralded by two odd-parity Z-checks, two defects. The error can be corrected by applying any small X-string which terminates at these defects. However, the mechanism described in II.D which applies an X correction at a fixed qubit for every defect, will have the effect of moving the single X-error around or it will create more X errors. It will utterly fail at removing errors. It is clear that an engineered dissipative dynamics should at

least correlate the parities of neighboring checks before applying any corrections. As an error string is only heralded by its two end-point defects, longer error strings require correlating the parity checks in a larger neighborhood, and hence more communication and delay in order to annihilate the error string. Said differently, one needs to dissipatively engineer the action of a non-local minimum-weight matching or RG decoder.

One can in fact view the classical non-local minimum-weight matching decoder as a source of computational power which jump-starts our quantum memory. Note that the RG decoder is non-local (even allowing for parallel processing of clusters on the lattice by local automata) as the maximum number of recursions r scales as $O(\log L)$ leading to a maximum cluster size proportional to the linear size of the lattice. The lowest levels of the RG decoder are of course local and will provide some measure of protection by local means. In (Harrington, 2004) the author devises an intricate scheme for doing purely local quantum error correction for the surface code by a 2D noisy cellular automaton assuming independent local errors; the mere existence of such a scheme is nontrivial as it has to deal with noise and communication delays.

It is important to contrast the challenge of physically engineering an on-chip decoder for the 2D surface code with the local decoder for the 4D toric code (Dennis *et al.*, 2002). In the 4D toric code an error cluster is surrounded by defect surfaces, in the way that a flipped spin-domain is surrounded by a domain wall in an 2D ferromagnetic Ising model. An error cluster can then be removed by locally shrinking the defect surface, i.e. there is a purely locally-defined "defect energy" function, requiring no communication over distances that depend on system size, whose minimization leads to the shrinking of the error cluster and thus to error correction. The absence of such local cost function is a generic property of 2D stabilizer codes and is directly related to the string-like nature of the error excitations which have observable defects only at their 0-dimensional boundary. It has been proven that all 2D stabilizer codes (Bravyi and Terhal, 2009) as well as generic 3D stabilizer codes (Yoshida, 2011) (but not all, see (Haah, 2011)) have string-like logical operators and this directly ties in with the lack of self-correction for these models.

1. Parity Check Measurements

In reality one should expect that parity check measurements are implemented as weak continuous measurements in time rather than a sequence of strong projective measurements. Examples of weak continuous qubit measurements are the measurement of a spin qubit in a semiconducting quantum dot through a quantum point contact (Elzerman *et al.*, 2003) and the measurement of a superconducting transmon qubit through homodyne measurement of a microwave cavity field with which it interacts. For short time scales such continuous weak measurements suffer from inevitable shot-noise as the current or voltage is carried by low numbers of quanta (electrons or photons); this noise averages out on longer times scales revealing the signal. The shot noise thus bounds the rate at which parity information can be gathered. The effect of leakage of qubits appears in such measurement traces either as a different output signal (detection of leakage) or, in the worst case, leads to a similar, and thus non-trustworthy, output signal which makes the parity check record unreliable for as long as a qubit occupies a leaked state.

The idea of realizing the surface code in superconducting circuit-QED systems using ancilla qubits for measurement laying out possible ways to couple qubits and resonators was considered in (DiVincenzo, 2009). A scalable surface code architecture was proposed and its basic unit, the Xmon, implemented in (Barends *et al.*, 2013) (see also (Barends *et al.*, 2014)). For the subsystem surface code, a possible layout of the elementary qubits for the subsystem surface code with superconducting transmon qubits coupled through resonators (including ancilla transmon qubits for measurement) was considered in (Huben, 2012).

In order to reduce qubit overhead and possibly make better use of the given physical interactions, e.g. cavity-atom (in cavity QED) or cavity-superconducting qubit (in circuit-QED) interactions, it is worthwhile to consider the idea of a *direct* parity check measurements instead of a parity measurement that is realized with several two-qubit gates and an ancilla as in Fig. 1. Any mechanism through which a probe pulse (modeled as a simple coherent state $|\alpha(t)\rangle$) picks up a π phase shift depending on a qubit state being $|0\rangle$ or $|1\rangle$ could function as the basis for such direct parity measurement. As long as the imprint of multiple qubits is through the addition of such phase shifts, we have $\alpha(t) \to \alpha(t)e^{i\pi P}$ where P is the parity of the qubits. Homodyne detection of such a probe pulse in time, that is, the continuous measurement of $\langle a(t) + a^\dagger(t)\rangle = (-1)^P 2\langle\alpha(t)\rangle$ (assuming $\alpha = \alpha^*$), could then realize a weak continuous parity measurement. This kind of set-up is natural for strong light-matter interactions in cavity-QED and circuit-QED where the state of the qubit can alter the refractive index of the medium (cavity) on which a probe pulse impinges. The challenge is to obtain phase shifts as large as π and ensure that these probe pulses do not contain more information about the qubits than their parity as this would lead to additional dephasing inside the odd/even parity subspace.

In the cavity-QED setting (Kerckhoff *et al.*, 2009) considered the realization of a continuous weak two-qubit parity measurement on two multi-level atoms each con-

tained in a different cavity (for possible improvements on this scheme, see (Nielsen, 2010)). Ref. (Lalumière *et al.*, 2010) considered a direct two-qubit parity measurement of two transmon qubits dispersively coupled to a single microwave cavity (circuit-QED setting). Similarly (DiVincenzo and Solgun, 2013) and (Nigg and Girvin, 2013) have considered direct 3 or more qubit parity check measurements for transmon qubits coupled to 2D or 3D microwave cavities.

(Kerckhoff *et al.*, 2010, 2011) have developed the interesting idea of a fully autonomous quantum memory which runs with fixed, time independent, input driving fields. In this approach, it is imagined that qubits are encoded in multi-level atoms coupled to the standing electromagnetic modes of (optical) cavities. Both Z- as well as X-parity checks of the qubits are continuously obtained via probe pulses applied to these cavities. These probe pulses are to be subsequently processed via photonic switches to coherently perform continuous quantum error correction.

IV. DISCUSSION

Physics in the past century has demonstrated the experimental viability of macroscopic quantum *states* such as the superconducting state or Bose-Einstein condensates. Quantum error correction which strives to preserve not a single macroscopic quantum state but the macroscopic states in a small subspace can be viewed as a natural but challenging extension to this. At the same time storing macroscopic quantum information is a first step towards the more ambitious goal of manipulating quantum information for computation purposes.

The current qubit realizations seem perhaps awkwardly suited to constitute the elementary qubits of an error-correcting code. Most elementary qubits are realized as *nondegenerate* eigenlevels (in a higher-dimensional space), approximately described by some $H_0 = -\frac{\omega}{2}Z$. The presence of H_0 immediately gives a handle on this qubit, i.e. processes which exchange energy with this qubit will drive it from $|1\rangle$ to $|0\rangle$ and vice versa (Rabi oscillations) and coupling of the qubit to other quantum degrees of freedom can be used for qubit readout. Passive (time-independent) interactions with other quantum systems are intentionally weak and only lead to significant multiple-qubit interactions if we supply energy in the form of time-dependent AC or DC fields meeting resonance conditions. To drive, keep or project multiple qubits via local parity checks in a code space where they are highly entangled, active control at the elementary qubit level will thus be continuously needed, making the macroscopic coding overhead look daunting. For such nondegenerate qubits typically all gates and preparation steps are only realized in *the rotating frame*, –the frame of reference in which the qubit state is no longer precessing around the z-axis on the Bloch-sphere due the presence of H_0. Any codeword $|\overline{\psi}\rangle$ is then only a fixed quantum state in this rotating frame while it is dynamically rotating under single-qubit Z rotations in the lab-frame. As measurements are only done in the lab-frame, it is only Z-measurements which can be done directly while X-measurements typically require an active rotation (e.g. Hadamard) followed by a Z-measurement. Once elementary qubits are used for times much longer than their coherence time, –when they are used together in a quantum memory–, the question of stability of this lab reference frame or the stability of the qubit frequency ω–, becomes important. Due to $1/f$ noise and aging of materials from which qubits are constructed, the qubit frequency ω can systematically drift over longer times and average to new values which are different from short time-averages. This has two consequences: one is that one needs to determine the qubit frequency periodically, for example by taking qubits periodically off-line and measuring them, so that one can re-calibrate gates whose implementation depends on knowing the rotating frame. Secondly, shifts in qubit frequency also induce shifts in coherence times as these times depend on the noise power spectral density $S(\omega)$ at the qubit frequency. Such fluctuations of coherence times over longer time-scales have been observed: as an example we can take the results in (Metcalfe *et al.*, 2007) which report that T_1 of a superconducting 'quantronium' qubit is changing every few seconds over a range of $1.4 - 1.8\mu$sec. It is clear that if elementary qubits are to be successfully used in a quantum memory then fluctuations of the noise rate have to be such that one remains below the noise threshold of the code that is employed in the memory at all times.

V. ACKNOWLEDGMENTS

I would like to thank Ben Criger for quickly making some of the figures and David DiVincenzo for interesting discussions and feedback on this review.

REFERENCES

Aharonov, D, and M. Ben-Or (1997), "Fault-tolerant quantum computation with constant error," in *Proceedings of 29th STOC*, pp. 176–188, `http://arxiv.org/abs/quant-ph/9611025`.

Aharonov, D, and L. Eldar (2011), "On the complexity of commuting local Hamiltonians, and tight conditions for topological order in such systems." in *Proceedings of FOCS 2011* (IEEE) pp. 334–343, `http://arxiv.org/abs/1102.0770`.

Aharonov, D, A. Kitaev, and J. Preskill (2006), "Fault-Tolerant Quantum Computation with Long-Range Correlated Noise," Phys. Rev. Lett. **96** (5), 050504.

Ahn, C, A. C. Doherty, and A. J. Landahl (2002), "Continuous quantum error correction via quantum feedback control," Phys. Rev. A **65** (4), 042301.

Alicea, J (2012), "New directions in the pursuit of Majorana fermions in solid state systems," Reports on Progress in Physics **75** (7), 076501, arXiv:1202.1293 [cond-mat.supr-con].

Alicki, R, M. Horodecki, P. Horodecki, and R. Horodecki (2008), "On thermal stability of topological qubit in Kitaev's 4D model," ArXiv e-prints arXiv:0811.0033 [quant-ph].

Aliferis, P (2007), *Level Reduction and the Quantum Threshold Theorem*, Ph.D. thesis (CalTech), `http://arxiv.org/abs/quant-ph/0703230`.

Aliferis, P, and A. Cross (2007), "Subsystem fault-tolerance with the Bacon-Shor code," Phys. Rev. Lett. **98**, 220502.

Aliferis, P, D. Gottesman, and J. Preskill (2006), "Quantum accuracy threshold for concatenated distance-3 codes," Quantum Info. and Comput. **6**, 97–165.

Aliferis, P, and J. Preskill (2009), "Fibonacci scheme for fault-tolerant quantum computation," Phys. Rev. A **79** (1), 012332.

Aoki, T, G. Takahashi, T. Kajiya, J.-i. Yoshikawa, S. L. Braunstein, P. van Loock, and A. Furusawa (2009), "Quantum error correction beyond qubits," Nature Physics **5**, 541.

Bacon, D (2006), "Operator quantum error correcting subsystems for self-correcting quantum memories," Physical Review A **73**, 012340.

Barends, R, J. Kelly, A. Megrant, D. Sank, E. Jeffrey, Y. Chen, Y. Yin, B. Chiaro, J. Mutus, C. Neill, P. O'Malley, P. Roushan, J. Wenner, T. C. White, A. N. Cleland, and J. M. Martinis (2013), "Coherent Josephson Qubit Suitable for Scalable Quantum Integrated Circuits," Physical Review Letters **111** (8), 080502, arXiv:1304.2322 [quant-ph].

Barends, R, J. Kelly, A. Megrant, A. Veitia, D. Sank, E. Jeffrey, T. C. White, J. Mutus, A. G. Fowler, B. Campbell, Y. Chen, Z. Chen, B. Chiaro, A. Dunsworth, C. Neill, P. O'Malley, P. Roushan, A. Vainsencher, J. Wenner, A. N. Korotkov, A. N. Cleland, and J. M. Martinis (2014), "Logic gates at the surface code threshold: Superconducting qubits poised for fault-tolerant quantum computing," ArXiv e-prints arXiv:1402.4848 [quant-ph].

Barreiro, J T, M. Müller, P. Schindler, D. Nigg, T. Monz, M. Chwalla, M. Hennrich, C. F. Roos, P. Zoller, and R. Blatt (2011), "An open-system quantum simulator with trapped ions," Nature **470**, 486–491.

Bombin, H (2010), "Topological subsystem codes," Phys. Rev. A **81** (3), 032301.

Bombin, H, G. Duclos-Cianci, and D. Poulin (2012), "Universal topological phase of two-dimensional stabilizer codes," New Journal of Physics **14** (7), 073048.

Bombin, H, and M. A. Martin-Delgado (2006), "Topological Quantum Distillation," Phys. Rev. Lett. **97** (18), 180501.

Bombin, H, and M. A. Martin-Delgado (2009), "Quantum measurements and gates by code deformation," Jour. of Phys. A: Math. Gen. **42** (9), 095302.

Braunstein, S (1998), "Error correction for continuous quantum variables," Phys. Rev. Lett. **80**, 4084.

Bravyi, S, G. Duclos-Cianci, D. Poulin, and M. Suchara (2013), "Subsystem surface codes with three-qubit check operators," Quantum Info. and Comput. **13** (11/12), 0963–0985.

Bravyi, S, and J. Haah (2013), "Analytic and numerical demonstration of quantum self-correction in the 3D Cubic Code," Phys. Rev. Lett. **111**, 200501.

Bravyi, S, and A. Kitaev (2005), "Universal quantum computation with ideal Clifford gates and noisy ancillas," Phys. Rev. A **71**, 022316.

Bravyi, S, and R. Koenig (2013), "Classification of topologically protected gates for local stabilizer codes," Phys. Rev. Lett. **110**, 170503.

Bravyi, S, B. Leemhuis, and B. M. Terhal (2011), "Topological order in an exactly solvable 3D spin model," Annals of Physics **326**, 839–866, arXiv:1006.4871 [quant-ph].

Bravyi, S, D. Poulin, and B. M. Terhal (2010), "Tradeoffs for Reliable Quantum Information Storage in 2D Systems," Phys. Rev. Lett. **104** (5), 050503.

Bravyi, S, and B. M. Terhal (2009), "A no-go theorem for a two-dimensional self-correcting quantum memory based on stabilizer codes," New Journal of Physics **11**, 043029.

Bravyi, S B, and A. Yu Kitaev (1998), "Quantum codes on a lattice with boundary," `http://arxiv.org/abs/quant-ph/9811052`.

Brooks, P, and J. Preskill (2013), "Fault-tolerant quantum computation with asymmetric Bacon-Shor codes," Phys. Rev. A **87** (3), 032310.

Bullock, S S, and G. K. Brennen (2007), "Qudit surface codes and gauge theory with finite cyclic groups," Jour. of Phys. A: Math. Gen. **40**, 3481–3505.

Castelnovo, C, and C. Chamon (2008), "Topological order in a three-dimensional toric code at finite temperature," Phys. Rev. B **78** (15), 155120, arXiv:0804.3591 [cond-mat.str-el].

Chase, B A, A. J. Landahl, and J. Geremia (2008), "Efficient feedback controllers for continuous-time quantum error correction," Phys. Rev. A **77** (3), 032304, arXiv:0711.0689 [quant-ph].

Cross, A W, D. P. DiVincenzo, and B. M. Terhal (2009), "A comparative code study for quantum fault tolerance," Quantum Info. and Comput. **9** (7), 541–572.

Denhez, G, A. Blais, and D. Poulin (2012), "Quantum-error-correction benchmarks for continuous weak-parity measurements," Phys. Rev. A **86** (3), 032318.

Dennis, E, A. Kitaev, A. Landahl, and J. Preskill (2002), "Topological quantum memory," J. Math. Phys. **43**, 4452–4505.

DiVincenzo, D P (2009), "Fault-tolerant architectures for superconducting qubits," Physica Scripta Volume T **137** (1), 014020.

DiVincenzo, D P, and F. Solgun (2013), "Multi-qubit parity measurement in circuit quantum electrodynamics," New Journal of Physics **15** (7), 075001.

Douçot, B, and L. Ioffe (2012), "Physical implementation of protected qubits ," Reports on Progress in Physics **75**, 072001.

Duclos-Cianci, G, and D. Poulin (2013), "Fault-Tolerant Renormalization Group Decoder for Abelian Topological Codes," ArXiv e-prints arXiv:1304.6100 [quant-ph].

Duclos-Cianci, G, and D. Poulin (2014), "Fault-Tolerant Renormalization Group Decoder for Abelian Topological Codes," Quantum Info. and Comput. **14** (9).

Duclos-Gianci, G, and D. Poulin (2010), "A renormalization group decoding algorithm for topological quantum codes," in *Proceedings of Information Theory Workshop (ITW)* (IEEE) pp. 1–5, `http://arxiv.org/abs/1006.1362`.

Edmonds, Jack (1965), "Paths, trees, and flowers," Canad. J. Math. **17**, 449–467.

Elzerman, J M, R. Hanson, J. S. Greidanus, L. H. Willems van Beveren, S. De Franceschi, L. M. K. Vandersypen, S. Tarucha, and L. P. Kouwenhoven (2003), "Few-electron

quantum dot circuit with integrated charge read out," Phys. Rev. B **67**, 161308.

Fowler, A G (2013), "Accurate simulations of planar topological codes cannot use cyclic boundaries," Phys. Rev. A **87**, 062320.

Fowler, A G, A. M. Stephens, and P. Groszkowski (2009), "High-threshold universal quantum computation on the surface code," Phys. Rev. A **80** (5), 052312.

Freedman, M H, and M. B. Hastings (2013), "Quantum Systems on Non-k-Hyperfinite Complexes: A Generalization of Classical Statistical Mechanics on Expander Graphs," ArXiv e-prints arXiv:1301.1363 [quant-ph].

Freedman, M H, and D. A. Meyer (2001), "Projective plane and planar quantum codes," Found. Comput. Math. **1** (3), 325–332, `http://arxiv.org/abs/quant-ph/9810055`.

Gladchenko, S, D. Olaya, E. Dupont-Ferrier, B. Douçot, L. B. Ioffe, and M. E. Gershenson (2009), "Superconducting nanocircuits for topologically protected qubits," Nature Physics **5**, 48–53, arXiv:0802.2295 [cond-mat.mes-hall].

Glancy, S, and E. Knill (2006), "Error analysis for encoding a qubit in an oscillator," Phys. Rev. A **73** (1), 012325.

Gottesman, D (1997), *Stabilizer Codes and Quantum Error Correction*, Ph.D. thesis (CalTech), `http://arxiv.org/abs/quant-ph/9705052`.

Gottesman, D (1999a), "Fault-Tolerant Quantum Computation with Higher-Dimensional Systems," Chaos, Solitons and Fractals **10**, 1749–1758, `http://arxiv.org/abs/quant-ph/9802007`.

Gottesman, D (1999b), "The Heisenberg Representation of Quantum Computers," in *Group22: Proceedings of the XXII International Colloquium on Group Theoretical Methods in Physics*, pp. 32–43, `http://arxiv.org/abs/quant-ph/9807006`.

Gottesman, D (2013), "What is the Overhead Required for Fault-Tolerant Quantum Computation?" ArXiv e-prints arXiv:1310.2984 [quant-ph].

Gottesman, D, and I. L. Chuang (1999), "Demonstrating the viability of universal quantum computation using teleportation and single-qubit operations," Nature **402**, 390–393.

Gottesman, D, A.Yu. Kitaev, and J. Preskill (2001), "Encoding a qubit in an oscillator," Phys. Rev. A **64**, 012310.

Guth, L, and A. Lubotzky (2013), "Quantum error-correcting codes and 4-dimensional arithmetic hyperbolic manifolds," ArXiv e-prints arXiv:1310.5555 [math.DG].

Haah, J (2011), "Local stabilizer codes in three dimensions without string logical operators," Phys. Rev. A **83** (4), 042330, arXiv:1101.1962 [quant-ph].

Haroche, S, M. Brune, and J.-M. Raimond (2007), "Measuring the photon number parity in a cavity: from light quantum jumps to the tomography of non-classical field states," Journal of Modern Optics **54** (13-15), 2101–2114.

Haroche, S, and J.-M. Raimond (2006), *Exploring the Quantum: Atoms, Cavities, and Photons* (Oxford Univ. Press, Oxford).

Harrington, J (2004), *Analysis of quantum error-correcting codes: symplectic lattice codes and toric codes*, Ph.D. thesis (CalTech), `http://thesis.library.caltech.edu/1747/`.

Horsman, C, A. G. Fowler, S. Devitt, and R. Van Meter (2012), "Surface code quantum computing by lattice surgery," New Journal of Physics **14** (12), 123011.

Huben, D (2012), "Geometric layouts of qubits for new lattice codes," Bachelor Thesis, RWTH Aachen (Supervision of D. P. DiVincenzo), available at JARA Institute for Quantum Information, Physics Dept., RWTH Aachen.

Jones, C (2013a), "Multilevel distillation of magic states for quantum computing," Phys. Rev. A **87**, 042305.

Jones, C (2013b), *Logic Synthesis for Fault-Tolerant Quantum Computers*, Ph.D. thesis (Stanford), `http://arxiv.org/abs/1310.7290`.

Katzgraber, H G, and R. S. Andrist (2013), "Stability of topologically-protected quantum computing proposals as seen through spin glasses," Journal of Physics Conference Series **473** (1), 012019, arXiv:1306.0540 [cond-mat.dis-nn].

Kerckhoff, J, L. Bouten, A. Silberfarb, and H. Mabuchi (2009), "Physical model of continuous two-qubit parity measurement in a cavity-QED network," Phys. Rev. A **79** (2), 024305, arXiv:0812.1246 [quant-ph].

Kerckhoff, J, H. I. Nurdin, D. S. Pavlichin, and H. Mabuchi (2010), "Designing Quantum Memories with Embedded Control: Photonic Circuits for Autonomous Quantum Error Correction," Physical Review Letters **105** (4), 040502, arXiv:0907.0236 [quant-ph].

Kerckhoff, J, D. S. Pavlichin, H. Chalabi, and H. Mabuchi (2011), "Design of nanophotonic circuits for autonomous subsystem quantum error correction," New Journal of Physics **13** (5), 055022, arXiv:1102.3143 [quant-ph].

Kitaev, A (2003), "Fault-tolerant quantum computation by anyons," Ann. Phys. **303**, 2–30.

Kitaev, A (2006), "Protected qubit based on a superconducting current mirror," `http://arxiv.org/abs/cond-mat/0609441`.

Kitaev, A Yu (1997), "Quantum computations: algorithms and error correction," Russian Math. Surveys **52**, 1191–1249.

Kitaev, Alexei (2006), "Anyons in an exactly solved model and beyond," Annals of Physics **321** (1), 2–111.

Knill, E (2005), "Quantum computing with realistically noisy devices," Nature **434**, 39–44.

Knill, E, R. Laflamme, and W. Zurek (1997), "Resilient quantum computation: Error models and thresholds," Proc. R. Soc. Lond. A **454**, 365–384.

Koch, J, Terri M. Yu, J. Gambetta, A. A. Houck, D. I. Schuster, J. Majer, A. Blais, M. H. Devoret, S. M. Girvin, and R. J. Schoelkopf (2007), "Charge-insensitive qubit design derived from the Cooper pair box," Phys. Rev. A **76**, 042319.

Koenig, R, G. Kuperberg, and B. W. Reichardt (2010), "Quantum computation with Turaev-Viro codes," Annals of Physics **325**, 2707–2749.

Kovalev, A A, and L. P. Pryadko (2013), "Fault tolerance of quantum low-density parity check codes with sublinear distance scaling," Phys. Rev. A **87** (2), 020304.

Kribs, D, R. Laflamme, and D. Poulin (2005), "Unified and Generalized Approach to Quantum Error Correction," Phys. Rev. Lett. **94** (18), 180501.

Lalumière, K, J. M. Gambetta, and A. Blais (2010), "Tunable joint measurements in the dispersive regime of cavity QED," Phys. Rev. A **81** (4), 040301.

Landahl, A J, J. T. Anderson, and P. R. Rice (2011), "Fault-tolerant quantum computing with color codes," `http://arxiv.org/abs/1108.5738`.

Leghtas, Z, G. Kirchmair, B. Vlastakis, R.J. Schoelkopf, M. H. Devoret, and M. Mirrahimi (2013), "Hardware-efficient autonomous quantum memory protection," Phys. Rev. Lett. **111**, 120501.

Leung, D W, M. A. Nielsen, I. L. Chuang, and Y. Yamamoto (1997), "Approximate quantum error correction can lead to better codes," Phys. Rev. A **56**, 2567–2573.

Levin, M A, and X.-G. Wen (2005), "String-net condensation: A physical mechanism for topological phases," Phys. Rev. B **71** (4), 045110.

Levy, J E, A. Ganti, C. A. Phillips, B. R. Hamlet, A. J. Landahl, T. M. Gurrieri, R. D. Carr, and M. S. Carroll (2009), "The impact of classical electronics constraints on a solid-state logical qubit memory," in *Proceedings of the 21st annual symposium on Parallelism in algorithms and architectures* (ACM, New York, NY, USA) pp. 166–168, `http://arxiv.org/abs/0904.0003`.

Lidar, D A (2012), "Review of Decoherence Free Subspaces, Noiseless Subsystems, and Dynamical Decoupling," ArXiv e-prints arXiv:1208.5791 [quant-ph].

Lidar, DA, and T.A. Brun, Eds. (2013), *Quantum Error Correction* (Cambridge University Press).

Lloyd, S, and J.-J. Slotine (1998), "Analog quantum error correction," Phys. Rev. Lett. **80**, 4088.

Menicucci, N C (2013), "Fault-tolerant measurement-based quantum computing with continuous-variable cluster states," ArXiv e-prints arXiv:1310.7596 [quant-ph].

Metcalfe, M, E. Boaknin, V. Manucharyan, R. Vijay, I. Siddiqi, C. Rigetti, L. Frunzio, R. J. Schoelkopf, and M. H. Devoret (2007), "Measuring the decoherence of a quantronium qubit with the cavity bifurcation amplifier," Phys. Rev. B **76**, 174516.

Mirrahimi, M, Z. Leghtas, V. V. Albert, S. Touzard, R. J. Schoelkopf, L. Jiang, and M. H. Devoret (2013), "Dynamically protected cat-qubits: a new paradigm for universal quantum computation," ArXiv e-prints arXiv:1312.2017 [quant-ph].

Müller, M, K. Hammerer, Y. L. Zhou, C. F. Roos, and P. Zoller (2011), "Simulating open quantum systems: from many-body interactions to stabilizer pumping," New Journal of Physics **13** (8), 085007.

Napp, J, and J. Preskill (2013), "Optimal Bacon-Shor codes," Quantum Info. and Comput. **13**, 490–510.

Ng, H K, and P. Mandayam (2010), "Simple approach to approximate quantum error correction based on the transpose channel," Phys. Rev. A **81** (6), 062342, arXiv:0909.0931 [quant-ph].

Nielsen, A E B (2010), "Fighting decoherence in a continuous two-qubit odd- or even-parity measurement with a closed-loop setup," Phys. Rev. A **81** (1), 012307, arXiv:0908.0817 [quant-ph].

Nielsen, M A, and I. L. Chuang (2000), *Quantum computation and quantum information* (Cambridge University Press, Cambridge, U.K.).

Nielsen, M A, and D. Poulin (2007), "Algebraic and information-theoretic conditions for operator quantum error-correction," Phys. Rev.A **75**, 064304(R).

Nigg, S E, and S. M. Girvin (2013), "Stabilizer quantum error correction toolbox for superconducting qubits," Phys. Rev. Lett. **110**, 243604.

Poulin, D (2005), "Stabilizer Formalism for Operator Quantum Error Correction," Phys. Rev. Lett. **95** (23), 230504.

Poulin, D (2006), "Optimal and efficient decoding of concatenated quantum block codes," Phys. Rev. A **74** (5), 052333.

Raussendorf, R, and J. Harrington (2007), "Fault-Tolerant Quantum Computation with High Threshold in Two Dimensions," Phys. Rev. Lett. **98** (19), 190504.

Raussendorf, R, J. Harrington, and K. Goyal (2007), "Topological fault-tolerance in cluster state quantum computation," New J. Phys. **9**, 199–219.

Shor, P W (1996), "Fault-tolerant quantum computation," in *Proceedings of 37th FOCS*, pp. 56–65.

Suchara, M, S. Bravyi, and B. Terhal (2011), "Constructions and noise threshold of topological subsystem codes," Jour. of Phys. A: Math. and Gen. **44** (15), 155301.

Suchara, M, A. Faruque, C.-Y. Lai, G. Paz, F. T. Chong, and J. Kubiatowicz (2013), "Comparing the Overhead of Topological and Concatenated Quantum Error Correction," ArXiv e-prints arXiv:1312.2316 [quant-ph].

Sun, L, A. Petrenko, Z. Leghtas, B. Vlastakis, G. Kirchmair, K. M. Sliwa, A. Narla, M. Hatridge, S. Shankar, J. Blumoff, L. Frunzio, M. Mirrahimi, M. H. Devoret, and R. J. Schoelkopf (2013), "Tracking Photon Jumps with Repeated Quantum Non-Demolition Parity Measurements," ArXiv e-prints arXiv:1311.2534 [quant-ph].

Svore, KM, D.P. DiVincenzo, and B.M. Terhal (2007), "Noise threshold for a fault-tolerant two-dimensional lattice architecture," Quantum Info. and Comput. **7**, 297–318.

Terhal, B M, F. Hassler, and D. P. DiVincenzo (2012), "From Majorana fermions to topological order," Phys. Rev. Lett. **108** (26), 260504.

Tillich, Jean-Pierre, and Gilles Zémor (2009), "Quantum LDPC codes with positive rate and minimum distance proportional to $n^{\frac{1}{2}}$," in *Proceedings of the IEEE Symposium on Information Theory*, pp. 799–803.

van Handel, R, and H. Mabuchi (2005), "Optimal error tracking via quantum coding and continuous syndrome measurement," eprint arXiv:quant-ph/0511221 quant-ph/0511221.

Vandersypen, L M K, and I. L. Chuang (2005), "NMR techniques for quantum control and computation," Rev. Mod. Phys. **76**, 1037–1069.

Vasconcelos, H, L. Sanz, and S. Glancy (2010), "All-optical generation of states for "Encoding a qubit in an oscillator"," Opt. Lett. **35** (3261–3263).

Wang, C, J. Harrington, and J. Preskill (2003), "Confinement-Higgs transition in a disordered gauge theory and the accuracy threshold for quantum memory," Annals of Physics **303**, 31–58.

Wang, D S, A. G. Fowler, A. M. Stephens, and L. C. L. Hollenberg (2009), "Threshold error rates for the toric and surface codes," ArXiv 0905.0531.

Weissman, M B (1988), "$1/f$ noise and other slow, nonexponential kinetics in condensed matter," Rev. Mod. Phys. **60**, 537–571.

Wiseman, H, and G.J. Milburn (2010), *Quantum Measurement and Control* (Cambridge University Press, Cambridge).

Wootton, J R (2012), "Quantum memories and error correction," Journal of Modern Optics **59**, 1717–1738.

Wootton, J R, J. Burri, S. Iblisdir, and D. Loss (2013), "Decoding non-Abelian topological quantum memories," ArXiv e-prints arXiv:1310.3846 [quant-ph].

Yao, X-C, T.-X. Wang, H.-Z. Chen, W.-B. Gao, A. G. Fowler, R. Raussendorf, Z.-B. Chen, N.-L. Liu, C.-Y. Lu, Y.-J. Deng, Y.-A. Chen, and J.-W. Pan (2012), "Experimental demonstration of topological error correction," Nature **482**, 489–494.

Yoshida, Beni (2011), "Feasibility of self-correcting quantum memory and thermal stability of topological order," Annals of Physics **326** (10), 2566 – 2633.

Zhang, J, C. Xie, K. Peng, and P. van Loock (2008), "Anyon statistics with continuous variables," Phys. Rev. A **78** (5), 052121.

Zhou, X, D. W. Leung, and I. L. Chuang (2000), "Methodology for quantum logic gate construction," Phys. Rev. A **62** (5), 052316.